AD-A059 718 GENERAL MOTORS CORP INDIANAPOLIS IND DETROIT DIESEL --ETC F/G 21/5
RESEARCH ON AEROELASTIC PHENOMENA IN THIN AIRFOIL CASCADES.(U)
AUG 78 S FLEETER N00014-72-C-0351

UNCLASSIFIED DDA-EDR-9575 NL

| OF |
AD
A059718

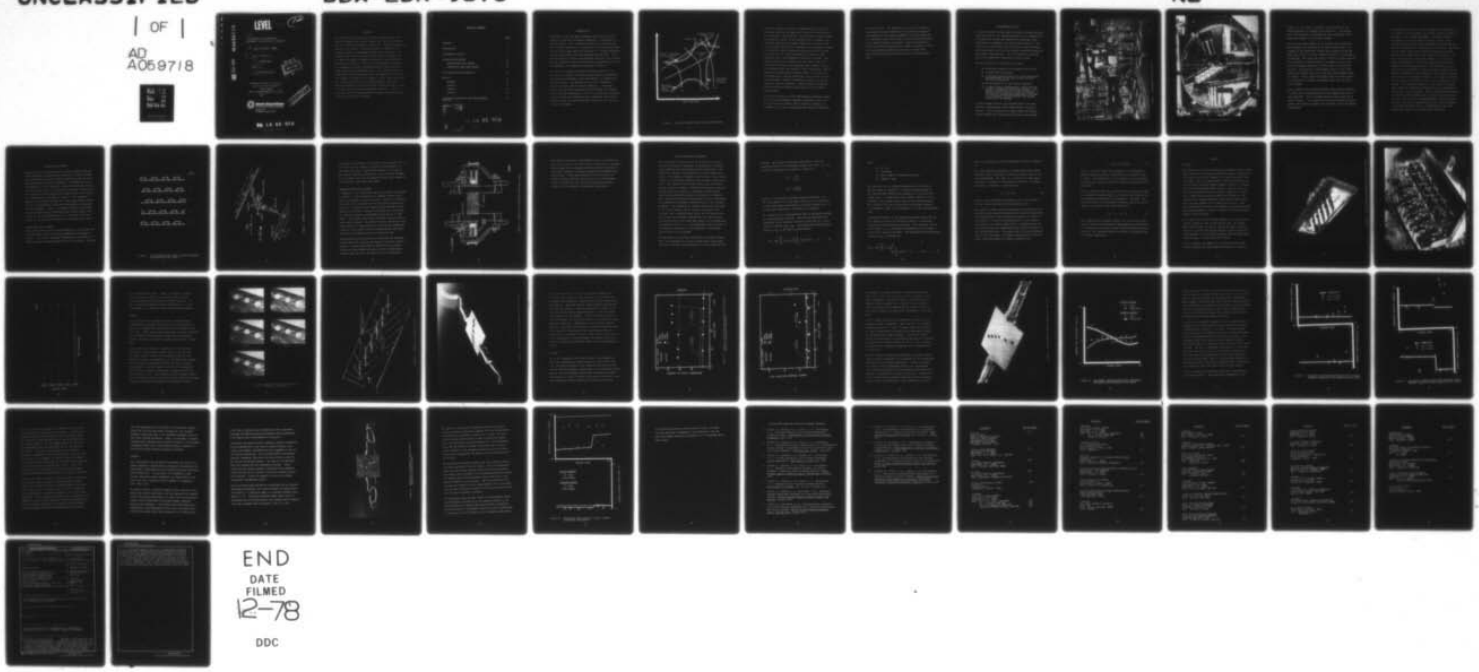

END
DATE
FILMED
12-78
DDC

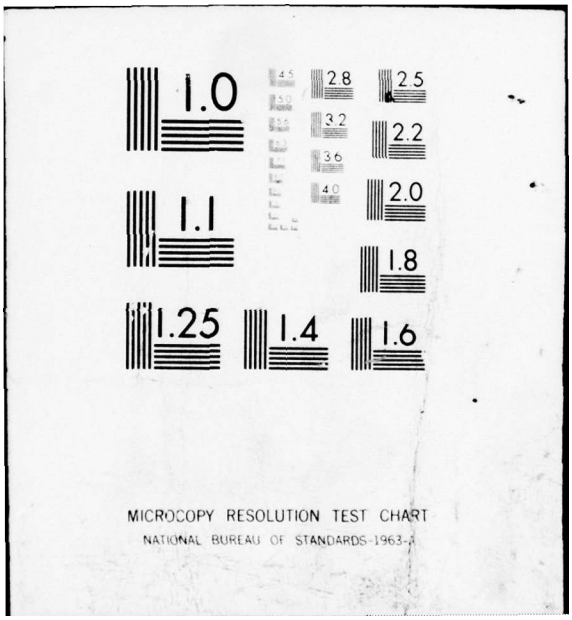
1.0
1.1
1.25
1.4
1.6
1.8
2.0
2.2
2.5
2.8
3.2
3.6
4.0
MICROCOPY RESOLUTION TEST CHART
NATIONAL BUREAU OF STANDARDS-1963-A

LEVEL II

AD A053931

12

6 RESEARCH ON AEROELASTIC PHENOMENA IN THIN AIRFOIL CASCADES.

9 FINAL SUMMARY REPORT,

14 DDA-EDR-9575

11 AUGUST 1978

12 56p.

10 SANFORD/FLEETER

RESEARCH SUPPORTED IN PART BY
OFFICE OF NAVAL RESEARCH
POWER BRANCH
UNDER CONTRACT N00014-72-C-0351
15

Detroit Diesel Allison
Division of General Motors Corporation
P.O. Box 894
Indianapolis, Indiana 46206

ABSTRACT

The advent of high tip-speed, high work, blading in the fan stages of advanced gas turbine engines has led to the recognition of a new type of blading instability – unstalled supersonic flutter. As a result, a concerted effort to develop an appropriate predictive mathematical model has taken place. To determine the range of validity and to direct refinements to the basic flow model, fundamental supersonic oscillating cascade data are required. This is the final summary report for an experimental research program directed at obtaining these unique time-variant aerodynamic data. The approach involved harmonically oscillating dynamically instrumented 2-D rectilinear cascades of airfoils in a supersonic inlet flow field, with the unsteady operation of the cascade computer controlled. Data were obtained in both torsion and translation over a range of steady and time-variant aerodynamic conditions. All of these data were then correlated with predictions obtained from a current state-of-the-art model.

TABLE OF CONTENTS

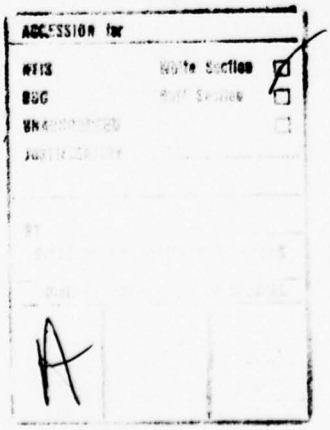

INTRODUCTION

The advent of the high-speed turbofan engine led to the discovery of a new type of blading instability — supersonic unstalled flutter. This instability, which until recently had been virtually unheard of, is defined as the self-excited vibration of rotor blades which are operating in a uniform supersonic relative inlet flow field with unstalled passage flow. It is characterized by a steep stress boundary and serves as a barrier for the high-speed, and even design point, operation of the fan or compressor, as schematically depicted in Figure 1.

To avoid this instability during the design process, it is necessary to calculate the time-variant pressure distributions (the unsteady aerodynamic forces and moments) on harmonically vibrating blades. The designer can use this information, together with the rotor structural damping, to accurately predict the supersonic unstalled flutter boundary of advanced design fans and compressors as well as to investigate alternate airfoil profiles and geometries which could move this flutter boundary beyond the engine operating regime prior to the fabrication of hardware.

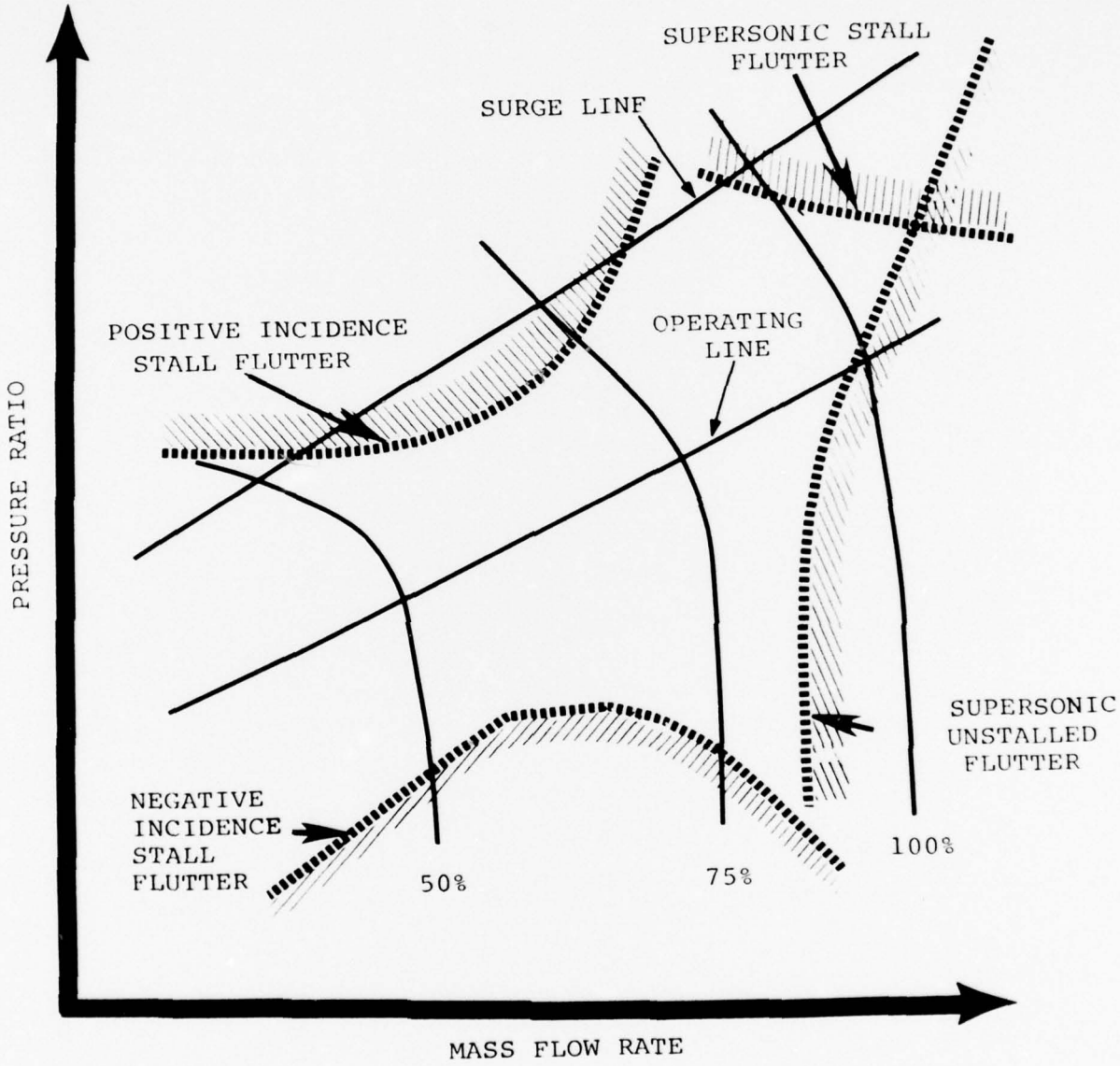

FIGURE 1. TYPES OF TURBINE ENGINE BLADE INSTABILITIES

Unstalled supersonic flutter is fundamentally an inviscid phenomena caused by the phase lag of the flow field relative to the motion of the airfoils. As this type of flutter tends to become more severe as the pressure ratio is lowered, the generally used analytical model assumes an inviscid, essentially supersonic flow with a subsonic axial component through a differential radial height fan stage operating at a pressure ratio of one. This differential fan stage is then developed into a two-dimensional rectilinear cascade. The cascade airfoils are assumed to be thin (most often zero thickness flat plates) and executing small harmonic torsion or translation mode oscillations. These assumptions lead to mathematical simplifications which result in a linearized, two-dimensional, constant coefficient (for the case of flat plate cascades), partial differential equation for the perturbation velocity potential. Various solution techniques have been and are currently being applied to this mathematical model.

The overall objective of this ONR sponsored research program was to obtain fundamental unsteady aerodynamic data to assess the range of validity and to indicate necessary refinements to the above noted basic math model for supersonic

unstalled flutter. The approach used in this experimental investigation involved harmonically oscillating dynamically instrumented 2-D rectilinear cascades of airfoils operating in a supersonic inlet flow field, with the unsteady operation of the cascade computer controlled. Data were obtained in both torsion and translation over a range of steady and time-variant aerodynamic conditions, with all of these data correlated with predictions from the state-of-the-art math model.

EXPERIMENTAL FACILITY

The Detroit Diesel Allison (DDA) rectilinear cascade facility, shown in Figure 2, was conceived and built as a research tool to evaluate the steady and time-variant aerodynamic characteristics of compressor and turbine blade sections. The facility is a continuous flow, non-return, pressure-vacuum type wind tunnel, with the test section evacuated by means of two primary steam ejectors. Up to 10 lbm/sec of filtered, dried, and temperature controlled air may be used.

The major features of this facility include

- Continuous operation for extended time periods.
- A mechanized test section.
- A schlieren optical system for visual observation and photography of the test section with the facility in operation.
- Bleed systems on all four tunnel sidewalls.
- A sophisticated instrumentation system centered around a laboratory-size digital computer. The computer provides on-line control of data acquisition, data reduction, calculates steady and time-variant cascade performance while the test is in progress, and also controls the dynamic operation of the cascade.

In this cascade facility, the entrance flow to the test section is generated by fixed nozzle blocks, as seen in Figure 3. The orientation of a sharp wedge with respect to this nozzle exit flow specifies the test section Mach

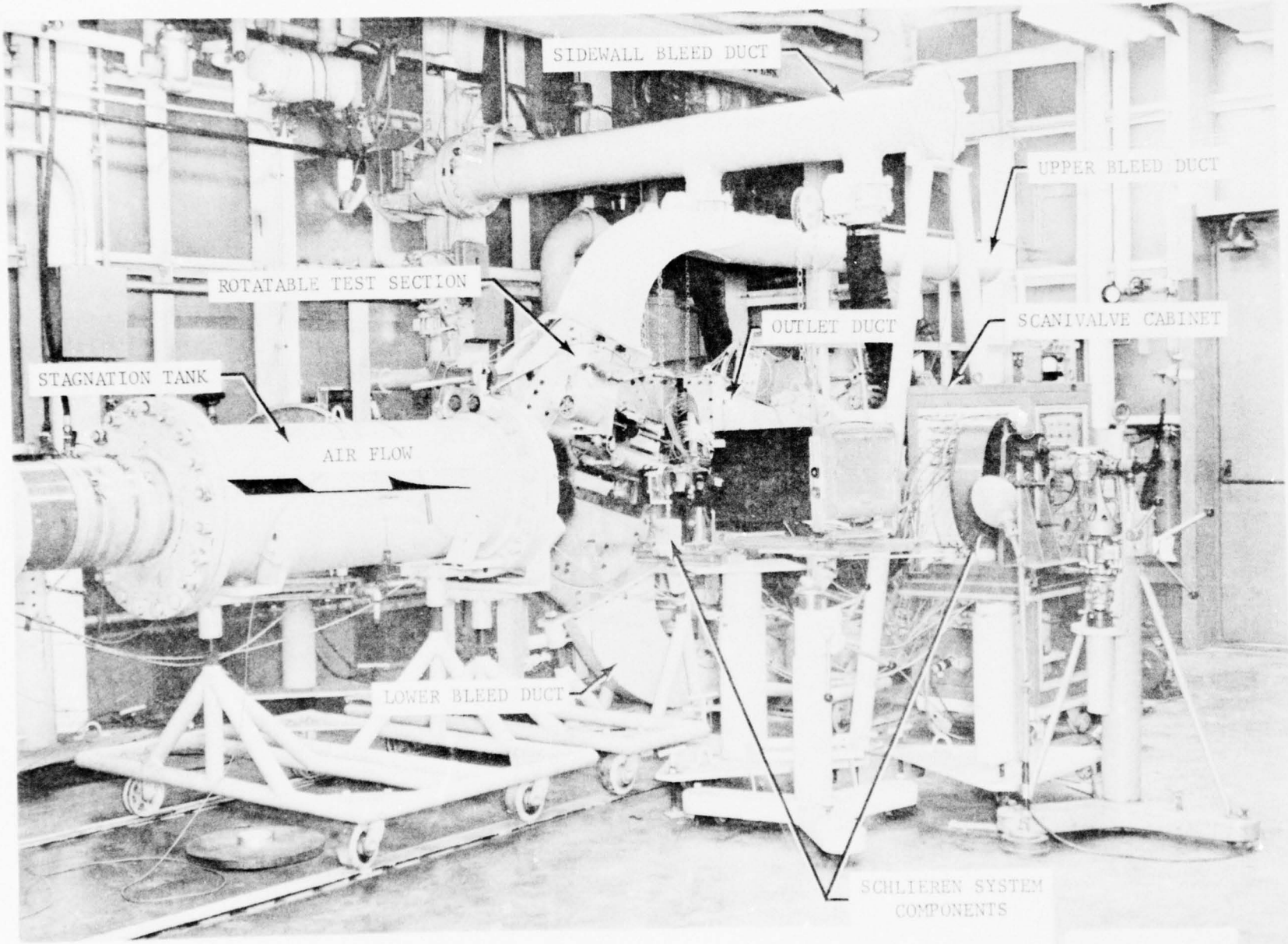

FIGURE 2. RECTILINEAR CASCADE FACILITY

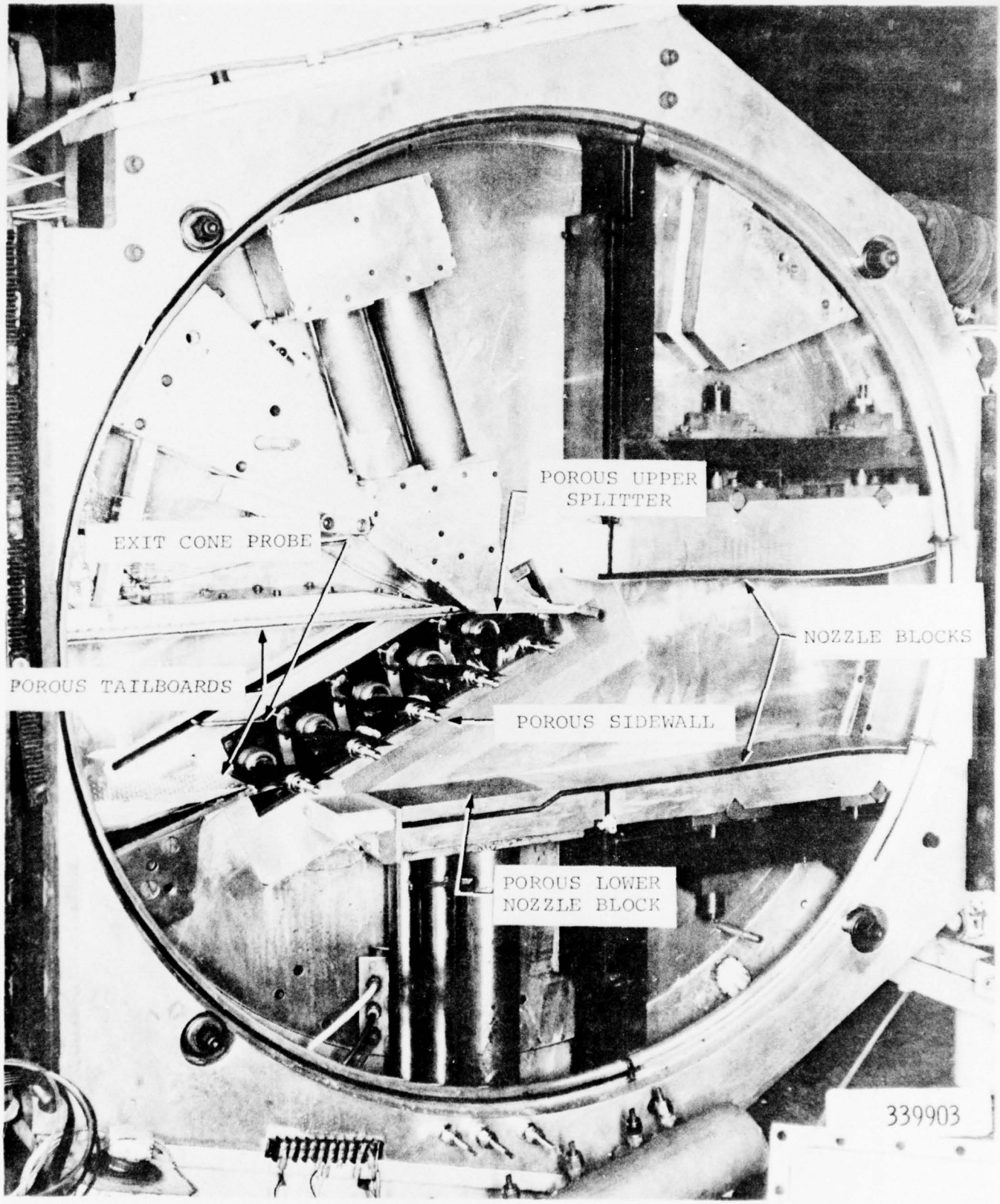

FIGURE 3. VIEW OF TEST SECTION

number, i.e. the shock or expansion wave generated by the wedge determines the cascade inlet conditions. The cascade inlet flow direction is determined by the orientation of the wedge with respect to the airfoil cascade.

To aid in the establishment of the cascade inlet periodicity, bleed chambers are provided on the lower nozzle block. Adjustment of the bleed rate through these chambers allows the inlet flow field to the rear (bottom) portion of the cascade to be affected. The inlet flow field to the front (upper) portion of the cascade is affected only by the wedge position, with the first passage controlled to some extent by the splitter position. The build-up of the boundary layer in this first passage can produce area ratios such that this passage cannot be started. Hence, bleed is provided along the front portion of the splitter to remove the boundary layer and start this first passage.

Active cascade inlet sidewall boundary layer control capability to assure the two-dimensionality of the cascade flow field is also available. This is accomplished with the suction strip seen in Figure 3. It contains five discrete regions yet still permits the schlieren system to be utilized to view the cascade wave system.

Disturbances generated at the lower endwall run downstream of the cascade in the supersonic flow regime and thus can have no influence on the cascade performance. The upper endwall of the tunnel, on the other hand, is crucial in that it can influence the whole flow field downstream of the cascade and prevent the formation of a periodic exit flow field. The shape of this upper endwall also uniquely determines the cascade pressure ratio under started exit operating conditions. The most crucial portion of the upper endwall is in the early stage of compression. Here the flow splitter provides the capability to both bleed and blow. This capability in conjunction with adjustments of the exit plenum pressure and the angle of attachment of the tailboard to the splitter, permits the setting of the streamline shape in this region and thereby sets the throttle condition to the first two channels of the cascade. The remaining problem is to not allow the cascade shock expansion system which impinges upon this tailboard to reflect back into the cascade. This is accomplished by making this upper tailboard porous with a 50% open area as well as having it open to the exit plenum pressure. This effectively produces a streamline representation of an infinite cascade at the design pressure ratio, as established in the first passage and results in a periodic exit flow field.

CASCADE DRIVE SYSTEMS

Dynamic testing to investigate and correctly simulate the cascade time-variant characteristics requires the airfoil cascade to be periodically excited at known frequencies with the interblade phase angle precisely controlled. To accomplish this, a 16K computer is used to generate a one-half square wave voltage signal for each airfoil at a specified excitation frequency with the required interblade phase angle imposed between the signals, as is schematically indicated in Figure 4. The cascade assemblies are designed such that the time-variant motion of each airfoil is controlled by individual electromagnets interfaced with this computer. Hence, the computer controls the harmonic airfoil oscillations by transmitting the one-half square wave signals to the electromagnets which in turn drive the airfoil cascade at the specified frequency and interblade phase angle.

TORSION MODE DRIVE SYSTEM

This research effort led to the development of a spring-bar torsion mode drive system of the type schematically depicted in Figure 5. An array of torsional frequencies is provided by attaching various thickness spring bars to the trunnions. Driving

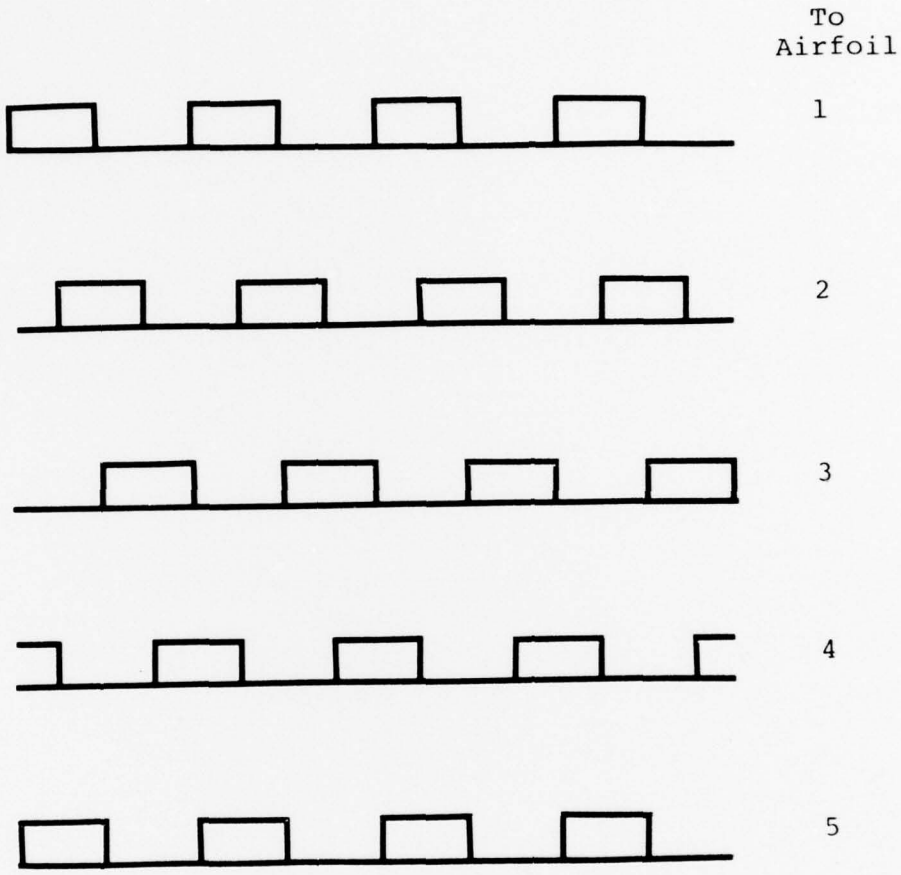

FIGURE 4. 90^{o} INTERBLADE PHASE ANGLE COMPUTER GENERATED SQUARE WAVE DRIVING SIGNAL

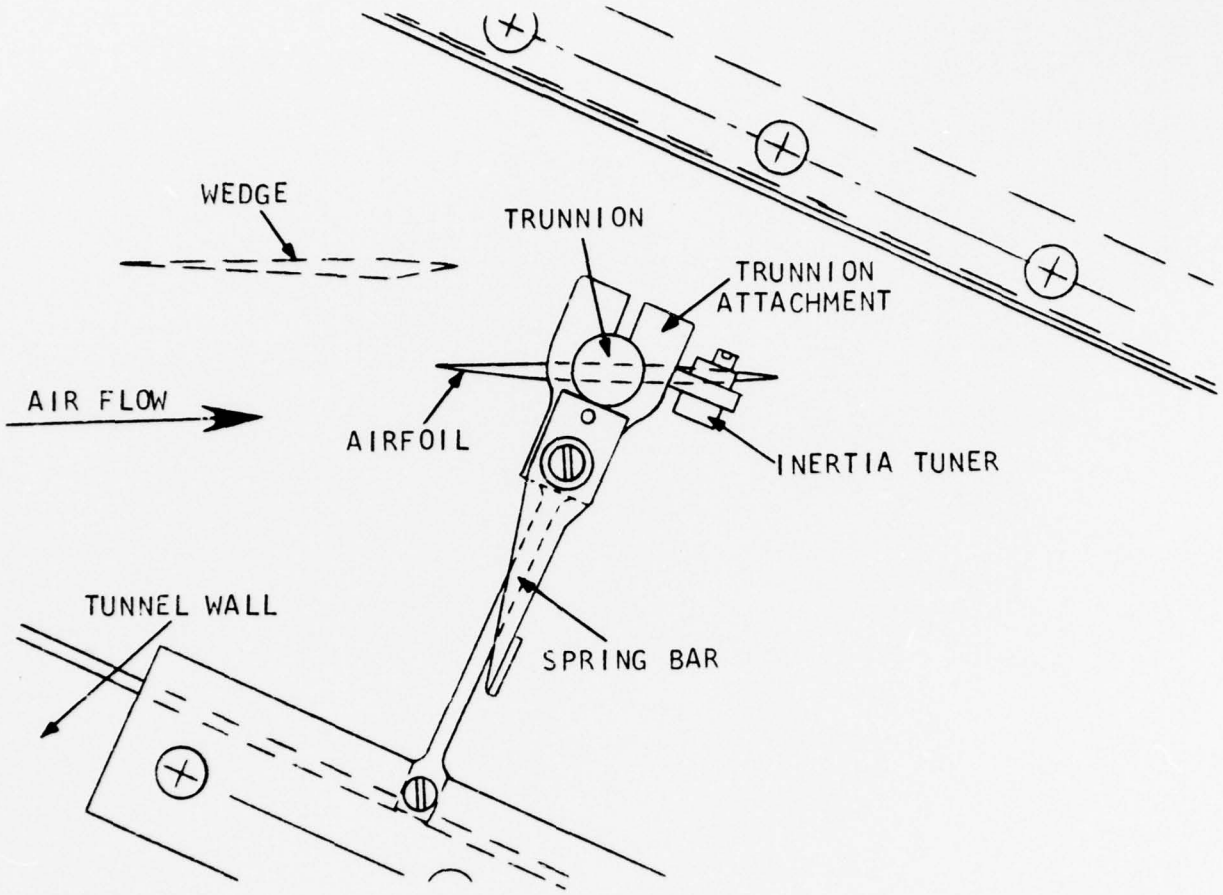

FIGURE 5. SCHEMATIC OF TORSION MODE DRIVE SYSTEM

mechanisms are attached to the airfoil trunnions which are in turn driven by the computer controlled electromagnets, as previously described. Strain gages mounted on the spring bars exhibit excellent sensitivity to the torsional movement of the airfoil, and allow the measured strain gage signals to be converted to rotational amplitudes.

TRANSLATION MODE DRIVE SYSTEM

A schematic of the translation mode drive system is presented in Figure 6. Since translation is movement normal to the chord, no bearing or other rigid axial restraint is necessary. The airfoil is positioned with the two flexible mounts consisting of a "squirrel cage" support which attaches to the spline on the airfoil trunnion by indexing over six grooves and attaching through a replaceable spring bar to a rigid mount. The indexing tabs ensure torsional restraint with no blade angle slippage. The airfoil trunnion splines are positioned axially on these devices by a driver arm clamped and piloted to the trunnion with an attached spacer tube which nests over the indexing tabs of the squirrel cage.

Translational excitation forces to each blade are supplied through the drive arm from the computer controlled electromagnets. Driving mechanisms are located on each airfoil trunnion so that proper excitation of the two-dimensional translational motion of the airfoil can be accomplished.

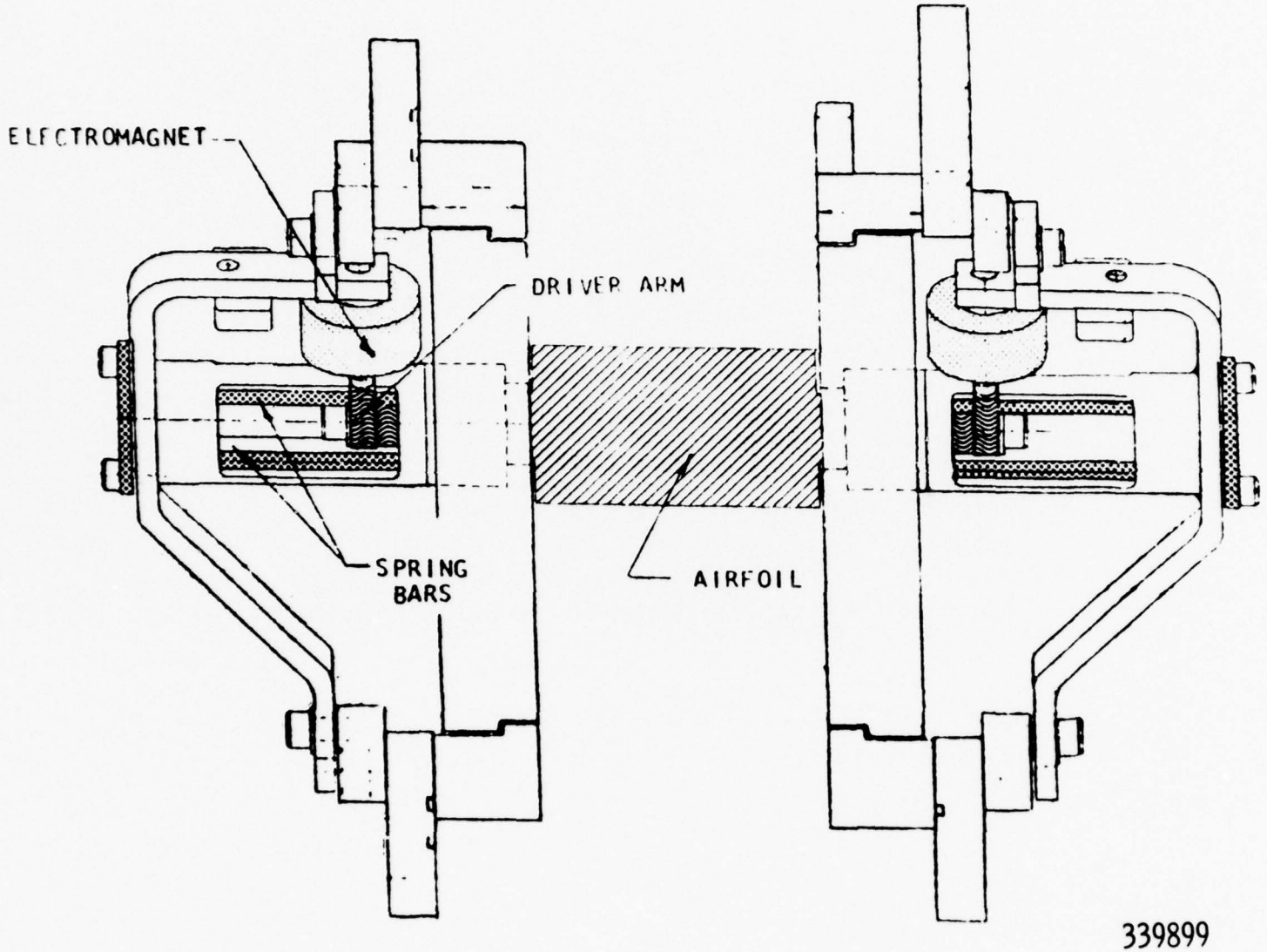

FIGURE 6. SCHEMATIC OF TRANSLATION MODE DRIVE SYSTEM

The computer controlled electromagnets excite the translation mode drive system at the airfoil-drive system natural frequency, thereby imparting the desired translation mode oscillation to the airfoil cascade at precisely controlled interblade phase angle values. Strain gages mounted on the spring bar assemblies exhibit excellent sensitivity to the translational airfoil oscillations, and allow the measured strain gage signals to be converted to translational amplitudes.

DATA ACQUISITION AND ANALYSIS

With the tunnel in operation and the steady-state cascade periodicity properly established, as determined by sidewall static pressure taps and schlieren flow visualization, the appropriate computer controlled drive system is made operational. This results in harmonic oscillations of the airfoil cascade at a prescribed frequency and interblade phase angle value. The resulting time-variant strain gage and airfoil surface pressure transducer signals are digitized at rates to 100,000 points per second by a 16-channel analog-digital converter and multiplexer system, and stored on a magnetic disk. These digitized data are analyzed on-line to determine the fundamental aerodynamic characteristics of the unsteady phenomena. The parameters of interest include the amplitude of the airfoil motion and the pressure disturbance, the frequency, the interblade phase angle, and the phase difference between the unsteady pressures and the airfoil motion as characterized by the strain gage signal on the dynamically instrumented airfoil, i.e., the aerodynamic phase lag data is referenced to the motion of the dynamically instrumented center airfoil in the cascade.

The amplitude of the airfoil motion and the pressure disturbance are determined by fitting a second order least square function to the data, differentiating it, and evaluating the

maximum. The pressure disturbance amplitude is then non-dimensionalized into an unsteady pressure coefficient, C_p, for torsion or translation, as defined in equation 1.

$$C_{p_\alpha} = \frac{p}{\frac{1}{2}\rho U^2 \alpha} \tag{1}$$

$$C_{p_T} = \frac{p}{\frac{1}{2}\rho U^2 \frac{h}{C}}$$

where p is the measured unsteady pressure amplitude, ρ is the fluid density, U is the inlet velocity, h/C is the ratio of the translational amplitude to the airfoil chord, and α is the torsional amplitude of oscillation (in radians).

The frequency of the time-dependent data is determined through the autocorrelation function. This function describes the dependence on the values of the data at one time, X_i, on the values at another time, X_{i+r}. The normalized autocorrelation function, R_{Xr}, is defined in series form as

$$R_{Xr} = \frac{1}{N-r} \sum_{i=1}^{N-r} X_i X_{i+r} \Big/ \frac{1}{N} \sum_{i=1}^{N} X_i X_i \quad r=0,1,2 \ldots m \tag{2}$$

where:

$X_i = X(i\ \Delta t)$

r = lag number

N = total number of dynamic data points

m = number of lags.

The lag time, Δt, is inversely proportional to the rate at which the data is digitized. A typical autocorrelogram of the digitized data exhibits the features of a sine wave plus random noise. A second order least square function is fit to the data in the second positive peak of the autocorrelogram. The inverse of the time at which this least square function is a maximum is equal to the frequency, f, of the time-dependent data.

The phase difference of the pressure disturbance along the airfoil chord in relation to the airfoil motion is calculated through the cross-correlation function. This function, for two sets of data, X_i, Y_i, describes the dependence of the values of one set of data on the other. The normalized cross-correlation function, R_{xyr}, is defined as:

$$R_{xyr} = \frac{1}{N-r} \sum_{i=1}^{N-r} X_i Y_{i+r} \Bigg/ \frac{1}{N} \sum_{i=1}^{N} X_i Y_i \qquad r = -m, \ldots -1,0,1, \ldots \quad (3)$$

where the variables are defined analogous to those in Equation (2).

As in the frequency calculation, a second order least square function is fit to the data in the first positive peak of the cross-correlogram. The time, t_p, at which this least square function is a maximum is analytically determined. The phase difference, in degrees, is calculated as

$$\theta_p = t_p \; f \; 360 \tag{4}$$

where f is the frequency calculated for the airfoil motion from the strain gage data, utilizing Equation (2).

Two sources of phase relation discrepancy are inherent in the electronic data acquisition system and correlation computation. The analog-digital (A/D) converter-multiplexer unit does not permit data to be digitized simultaneously on all channels. Consequently, an inherent phase shift is introduced into the physical data when the cross-correlation function operates on the raw digitized data. This phase shift, for the sinusoidal data in this experiment, is directly proportional to the "cut rate" of the multiplexer, as shown in Equation (5):

$$\theta_s = f_x(K_y - K_x)\ 360/R_a \qquad (5)$$

where θ_s is the AD phase shift inherent in the computation between channels K_y and K_x, representing the respective data, Y_i and X_i. The frequency, f_x, corresponds to the disturbance in channel K_x, and R_a is the rate at which the data were being digitized.

Prior to acquiring data the electronic data acquisition system is calibrated for phase shift, θ_a, using the A/D converter and the computation described in the foregoing. Therefore, the phase difference of the pressure disturbance along the airfoil surface in relation to the airfoil motion is

$$\theta_{xy} \approx \theta_p - \theta_s - \theta_a \ . \qquad (6)$$

This computational procedure results in a valid on-line data analysis system and provides the experimentalist with meaningful information with which to make judicious decisions during the test. All analyzed results are stored on a magnetic disk for further examination.

RESULTS

CASCADE 1

The objective of the initial cascade investigation was to demonstrate the ability to achieve controlled harmonic torsional oscillations of an airfoil cascade in a steady supersonic inlet flow field. This was accomplished by developing and applying the previously described dynamic computer system to a cascade of five flattened double-wedge airfoils. Each of these airfoils was cantilevered from a trunnion attached to a torsion rod. A double-pass schlieren system was provided for flow visualization, accomplished with a back surface glass mirror inset into one sidewall of the tunnel test section. Each cantilevered airfoil-torsion rod assembly was inserted through the mirrored sidewall, as seen in Figure 7, with the trunnion mounted on ball bearings.

On the back side of the mirrored sidewall, an airfoil driving arm was attached to each of the torsion rods. An electromagnet was provided for each of the driving arms, as seen in Figure 8, to permit the on-line computer system to drive the electromagnets at a prescribed frequency and interblade phase angle and they, in turn, drive the airfoils.

Figure 9 presents an example of the digitized strain gage signals obtained with the cascade oscillating in torsion in

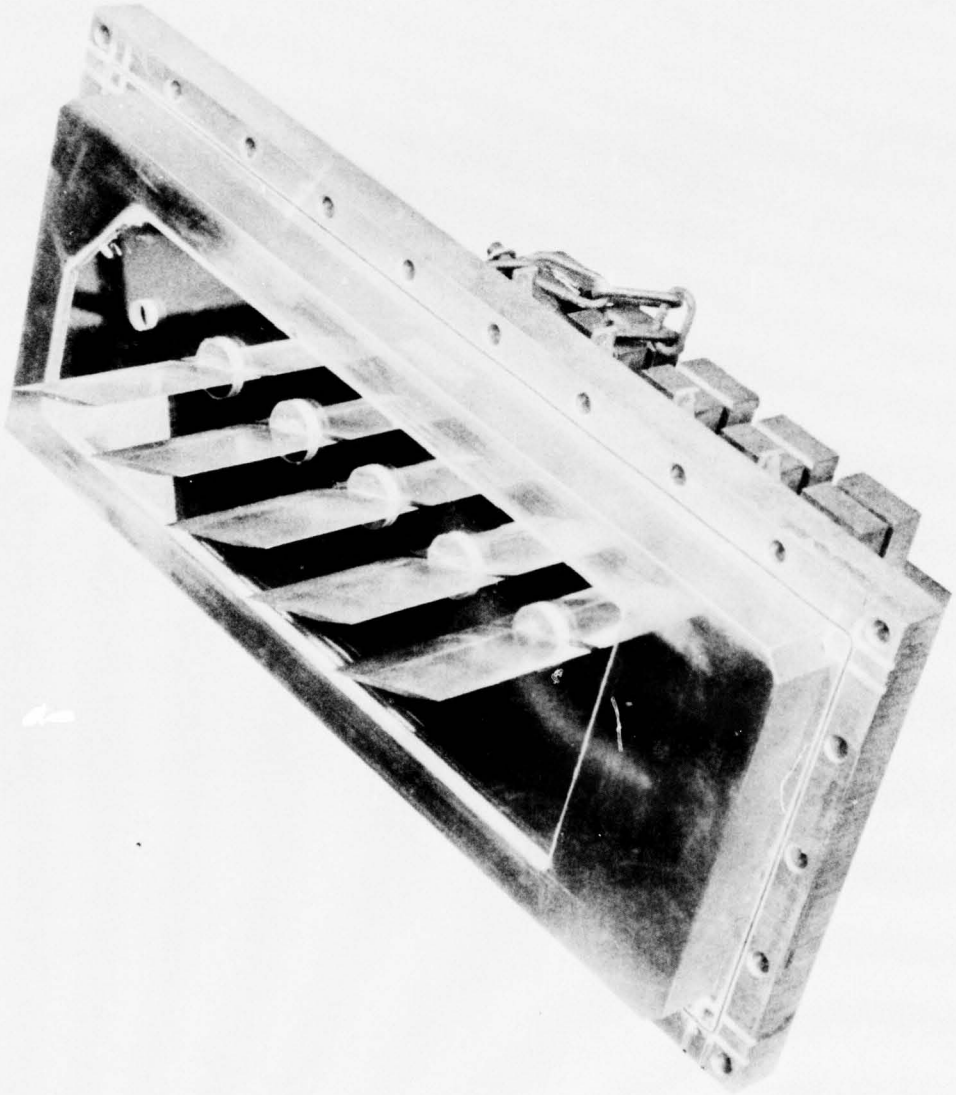

FIGURE 7. AIRFOIL CASCADE CANTILEVERED FROM MIRRORED SIDEWALL

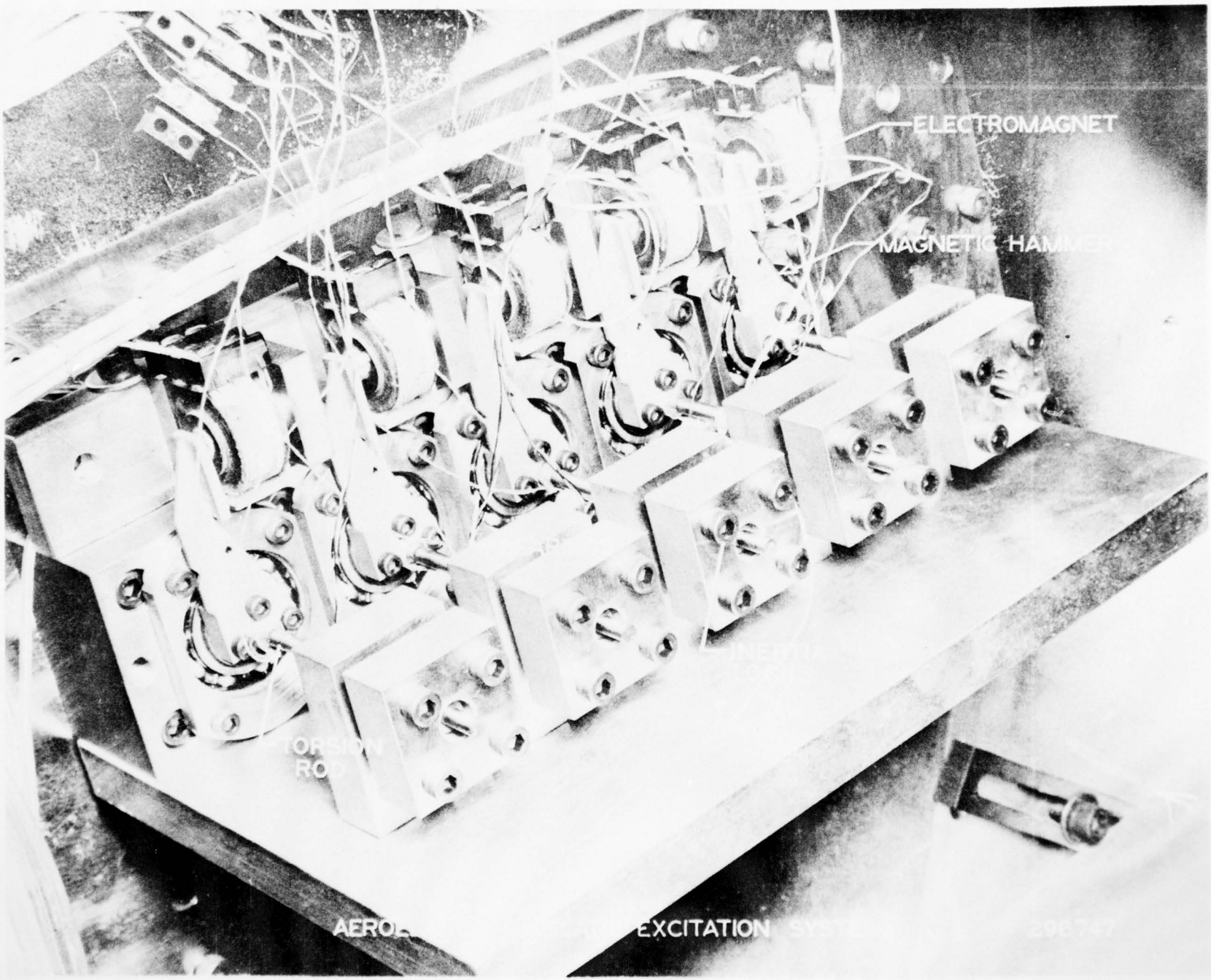

FIGURE 8. CASCADE TORSION ROD DRIVE SYSTEM

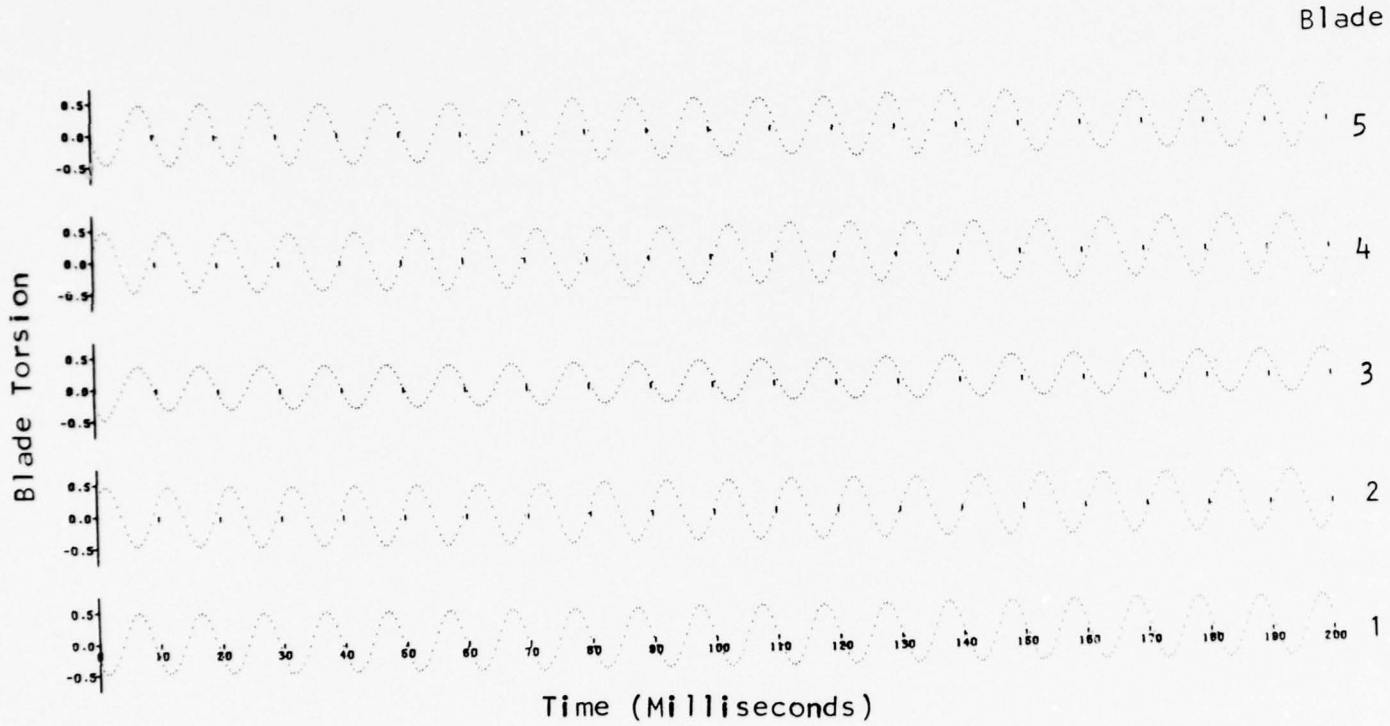

FIGURE 9. TYPICAL DIGITIZED STRAIN GAGE SIGNALS

the supersonic wind tunnel. Figure 10 presents a sequence from a high-speed schlieren movie which shows the time-variant phenomena during controlled cascade operation. As seen, controlled harmonic torsional oscillations of an airfoil cascade in a supersonic flow field have been achieved.

CASCADE 2

The objective of this unsteady cascade investigation was to quantitatively measure the time-variant pressure distribution on an harmonically oscillating airfoil cascade for the first time. These unique torsion mode data were then correlated with predictions obtained from a state-of-the-art analysis, thereby indicating its range of validity and necessary refinements.

A classical airfoil profile, consisting of a flat suction surface and a wedge-shaped pressure surface, was selected. The center (third) airfoil of the cascade, Figure 11, was machined to permit the embedding of 11 miniature high response dynamic pressure transducers such that the airfoil contour was preserved. Figure 12 shows a view of this instrumented airfoil with the pressure transducers, staggered across the span, clearly visible. These double-trunnion cascade airfoils were then mounted using the spring bar torsion mode drive system previously described and schematically depicted in Figure 5.

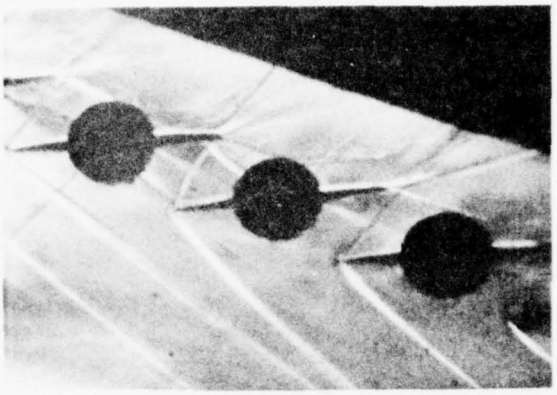

NO. 1

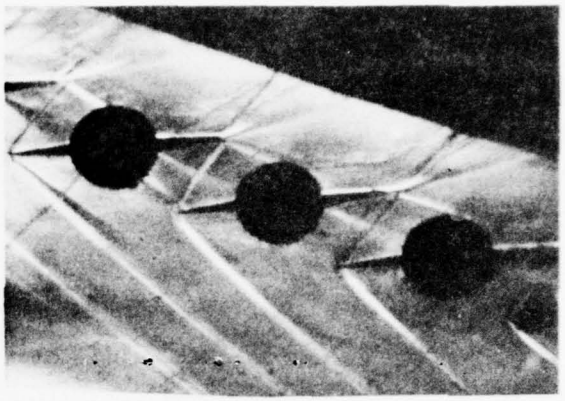

NO. 4

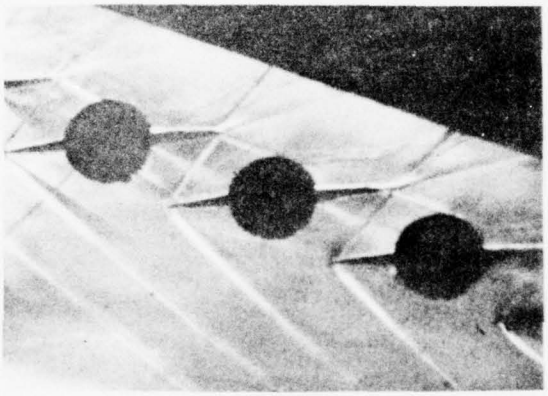

NO. 2

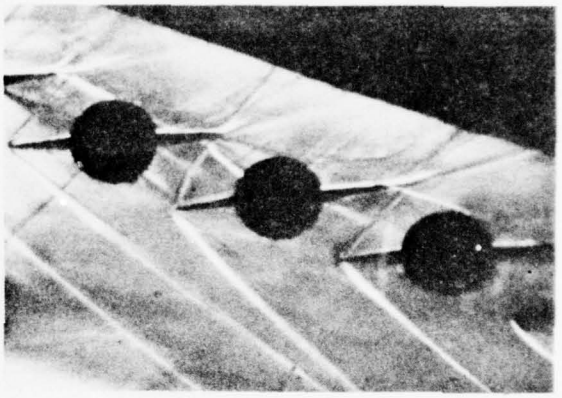

NO. 5

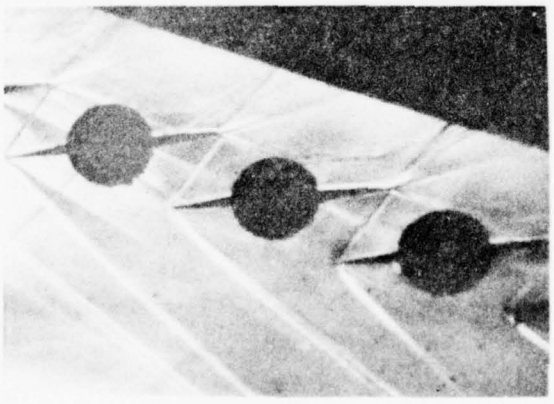

NO. 3

FIGURE 10. SEQUENCE FROM HIGH-SPEED SCHLIEREN MOVIE FOR 180° INTERBLADE PHASE ANGLE

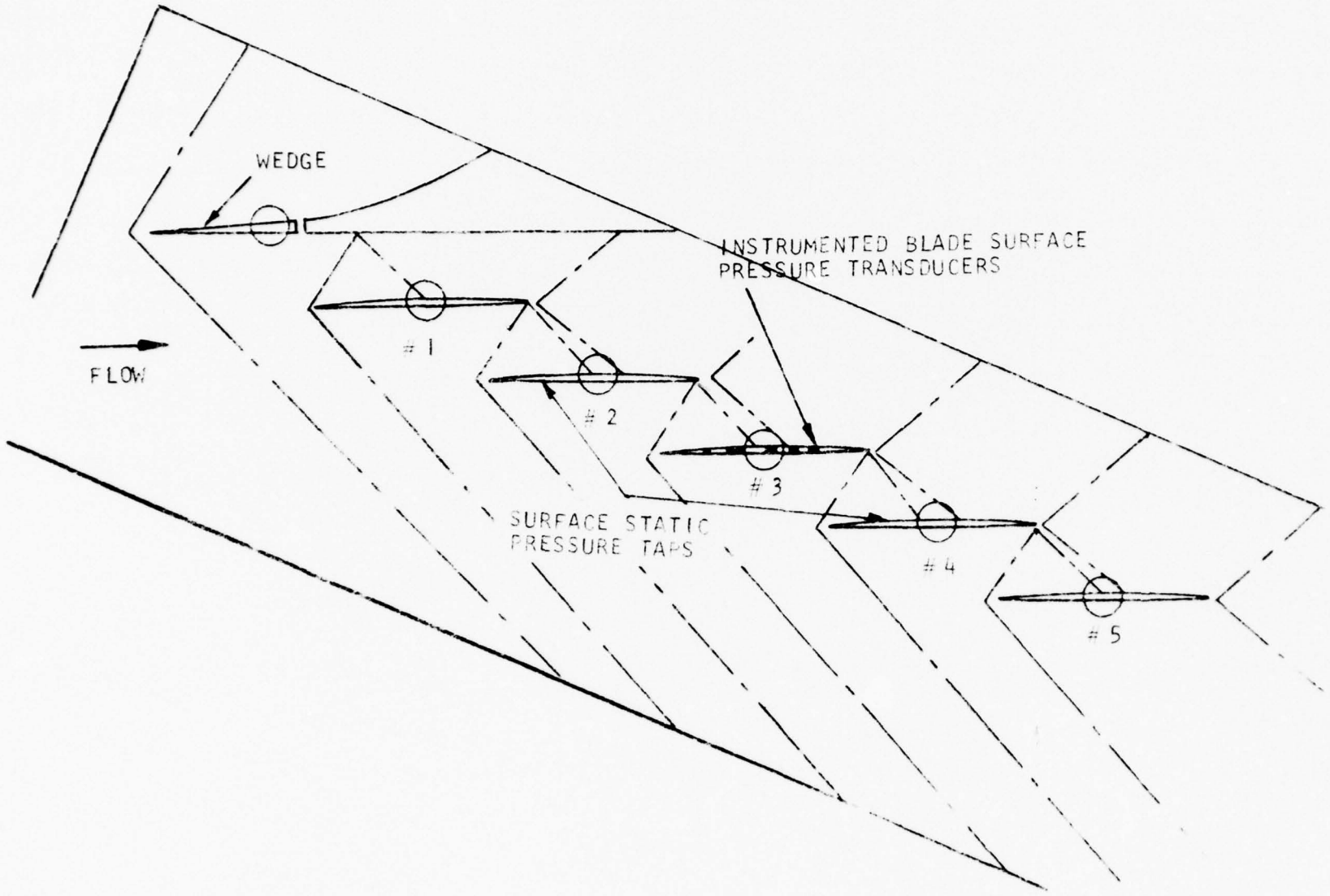

FIGURE 11. SCHEMATIC OF CASCADE FLOW FIELD

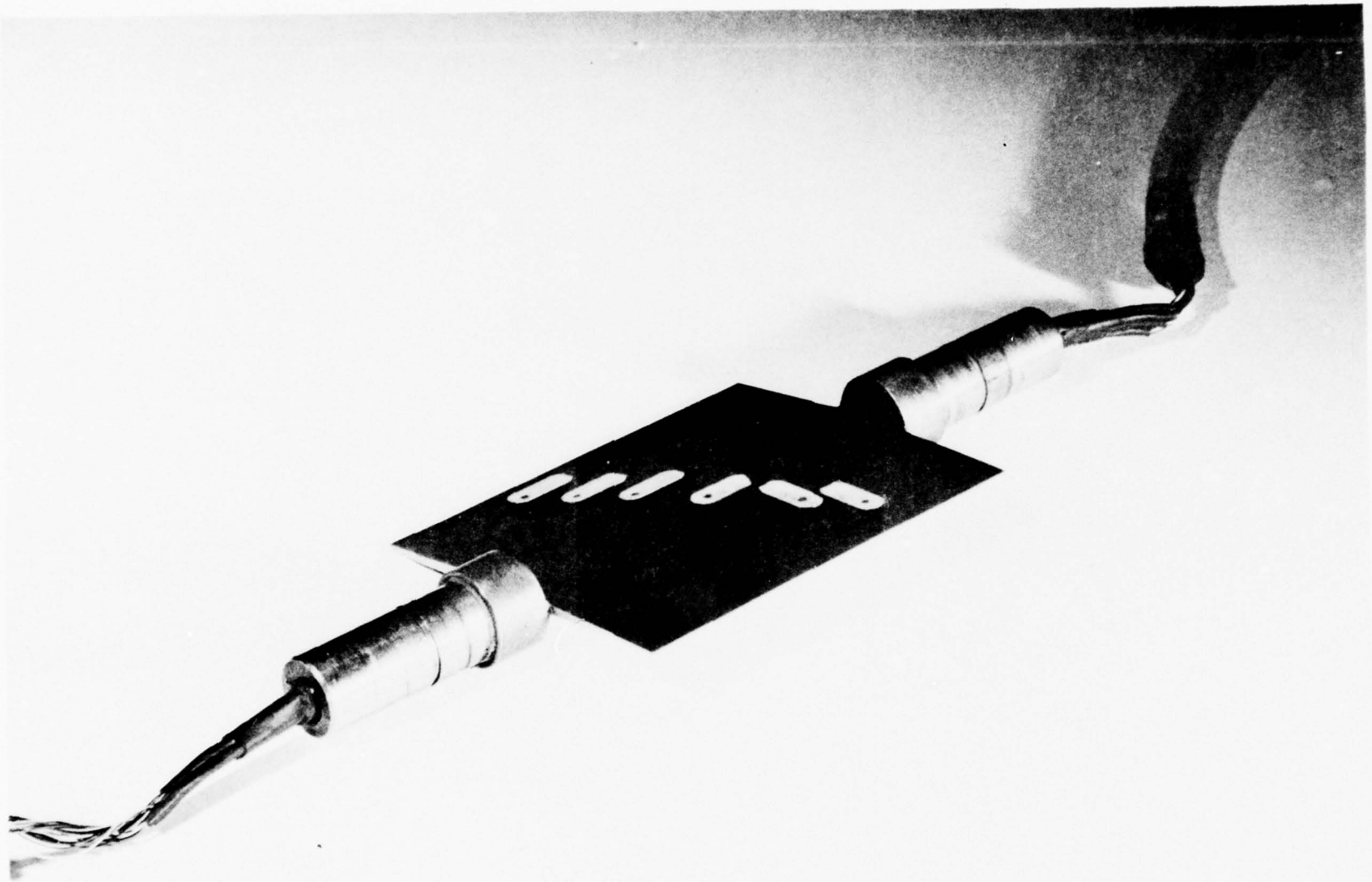

FIGURE 12. PRESSURE SURFACE OF INSTRUMENTED CLASSICAL AIRFOIL

Data were obtained over a range of inlet Mach numbers and interblade phase angles for two torsional axis locations and correlated with analytical results from a current state-of-the-art analysis. These data did not always exhibit good correlation with the analysis. This was shown to be a result of the variation of the blade-to-blade amplitude, an effect heretofore neglected in the analyses. All of the state-of-the-art analyses consider the oscillating blades to be undergoing equal amplitude vibrations. Modification of the state-of-the-art analysis to include this variation in blade-to-blade amplitude led to excellent correlation of the experimental data, as clearly seen in Figures 13 and 14. This is felt to be a significant advancement in the development of analyses which will predict the unsteady aerodynamic forces on fan and compressor blades.

CASCADE 3

One of the fundamental differences between the mathematical model and turbomachinery design practice is the airfoil loading. The model considers a zero thickness flat plate airfoil cascade executing harmonic oscillations in a uniform flow field. However, fan and compressor blades have thickness and camber and operate at a static pressure ratio greater than unity, with the aerodynamic loading affecting the overall steady-state

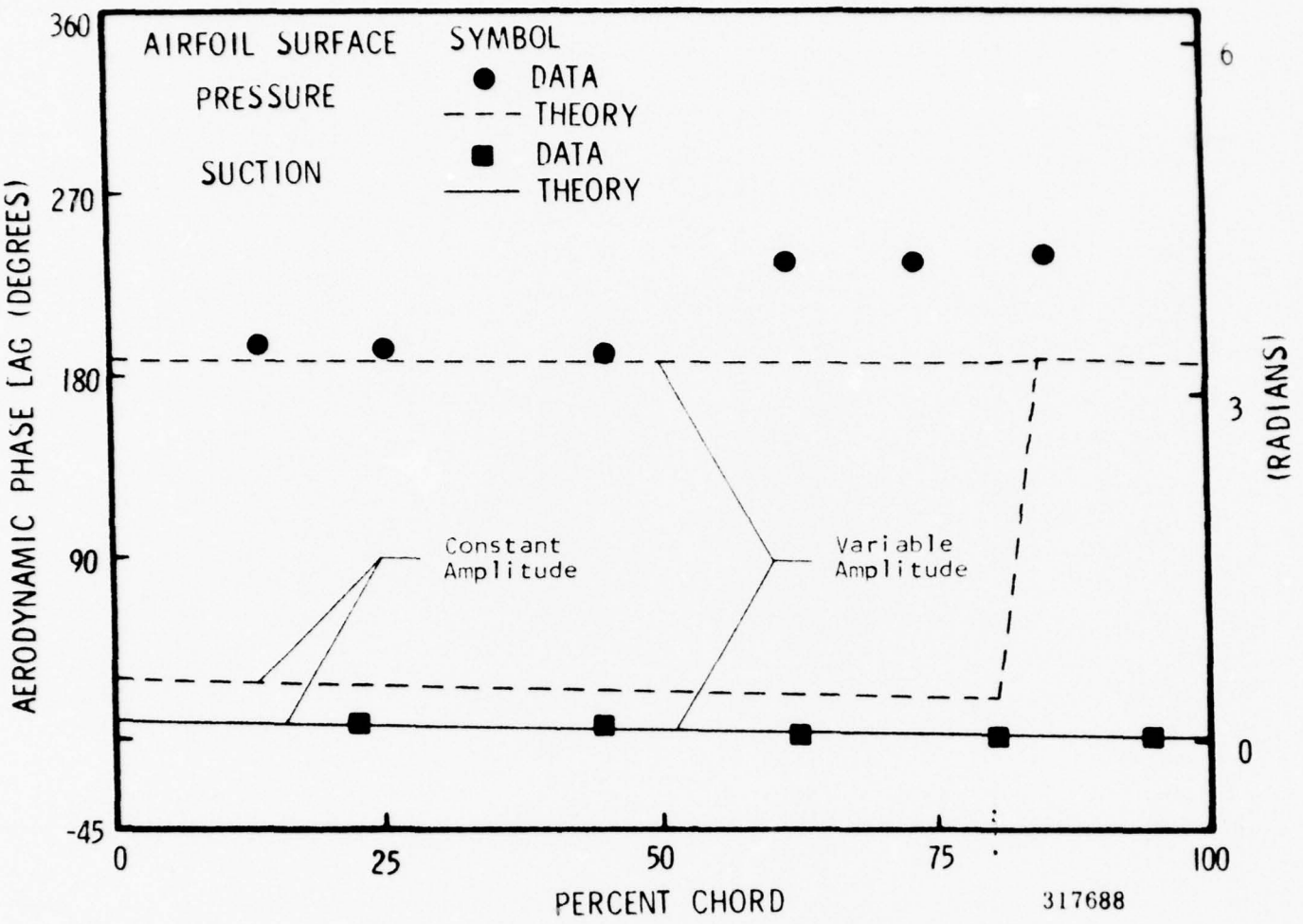

FIGURE 13. CLASSICAL AIRFOIL CASCADE TORSION MODE AERODYNAMIC PHASE LAG DATA-THEORY CORRELATION

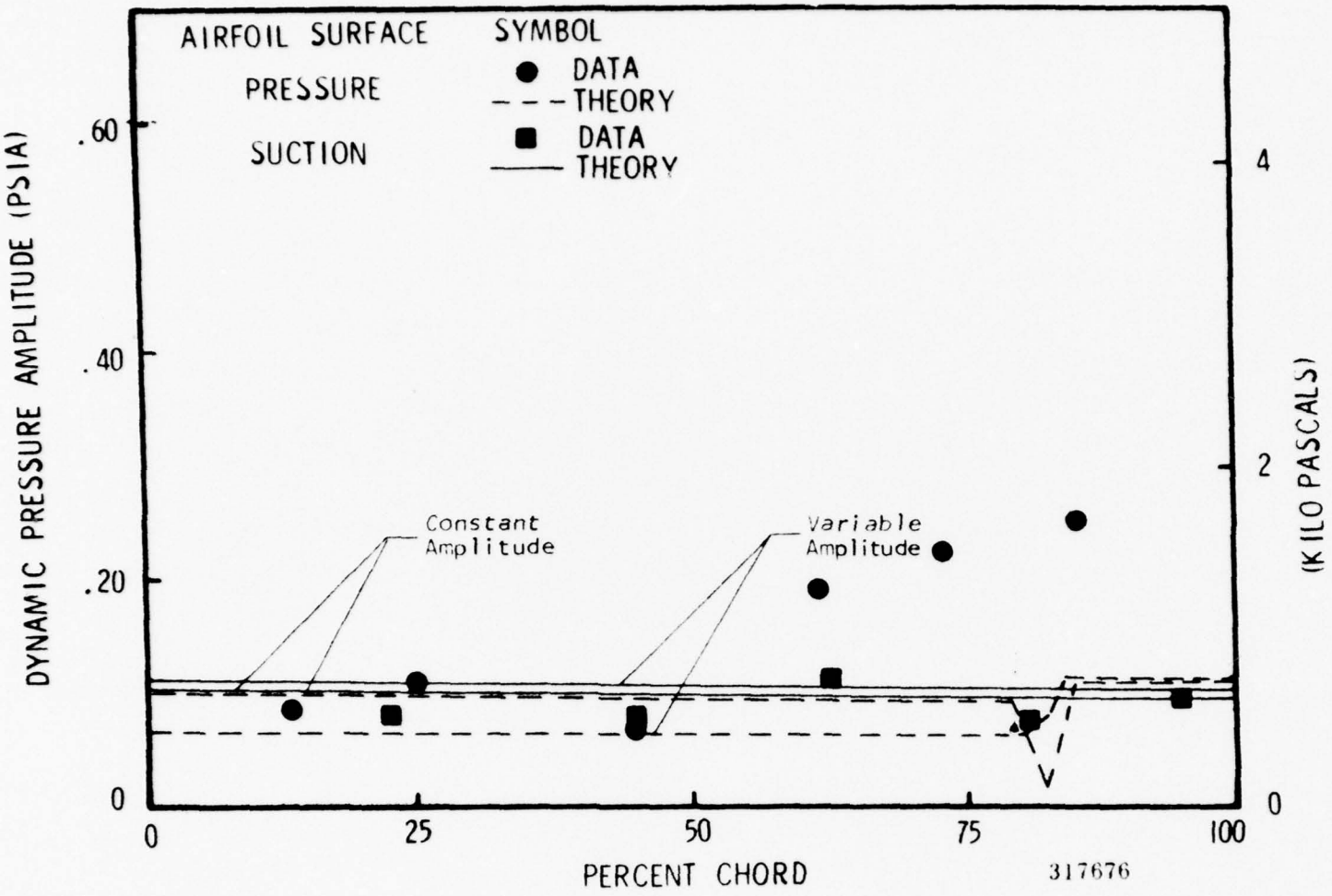

FIGURE 14. CLASSICAL AIRFOIL CASCADE TORSION MODE DYNAMIC PRESSURE AMPLITUDE DATA-THEORY CORRELATION

aerodynamics, including the shock structure and wake characteristics. Hence, the objective of this experiment was to obtain fundamental time-variant data on an advanced design cambered airfoil cascade over a range of static pressure ratios to quantitatively demonstrate the apparent deficiencies and to indicate the significant refinements to the basic model.

Figure 15 shows the MCA airfoil embedded with Kulite, high-response pressure transducers. Note that this is a uniquely instrumented airfoil. First, increased sensitivity Kulites are used, accomplished by decreasing the diaphragm thickness and increasing the bridge impedence. Second, the airfoil contour was maintained to an extremely high degree of accuracy by staggering the Kulites and by the use of a thin, pliable coating over the transducer diaphragm, with no depreciation in sensitivity.

With the cascade periodicity established, the steady cascade airfoil surface performance was determined for the aerodynamic conditions of the unsteady experiments. Figure 16 presents the airfoil surface performance data for the low pressure ratio condition together with the predictions obtained from a transonic, time-marching, steady flow analysis. Overall the airfoil steady surface pressure distribution data correlates very well with the predictions. The correlation is not as

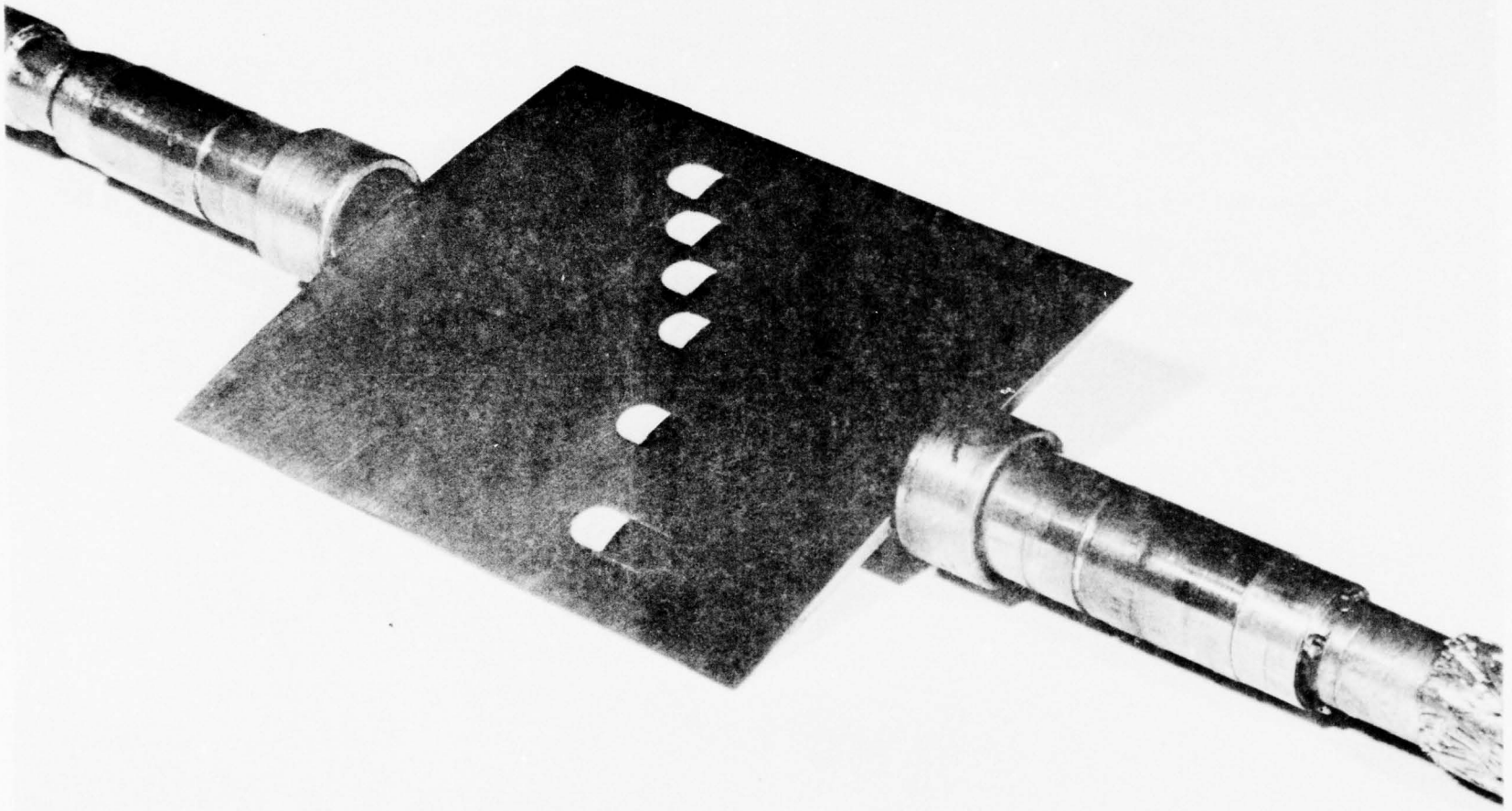

FIGURE 15. INSTRUMENTED MULTIPLE CIRCULAR ARC (MCA) AIRFOIL

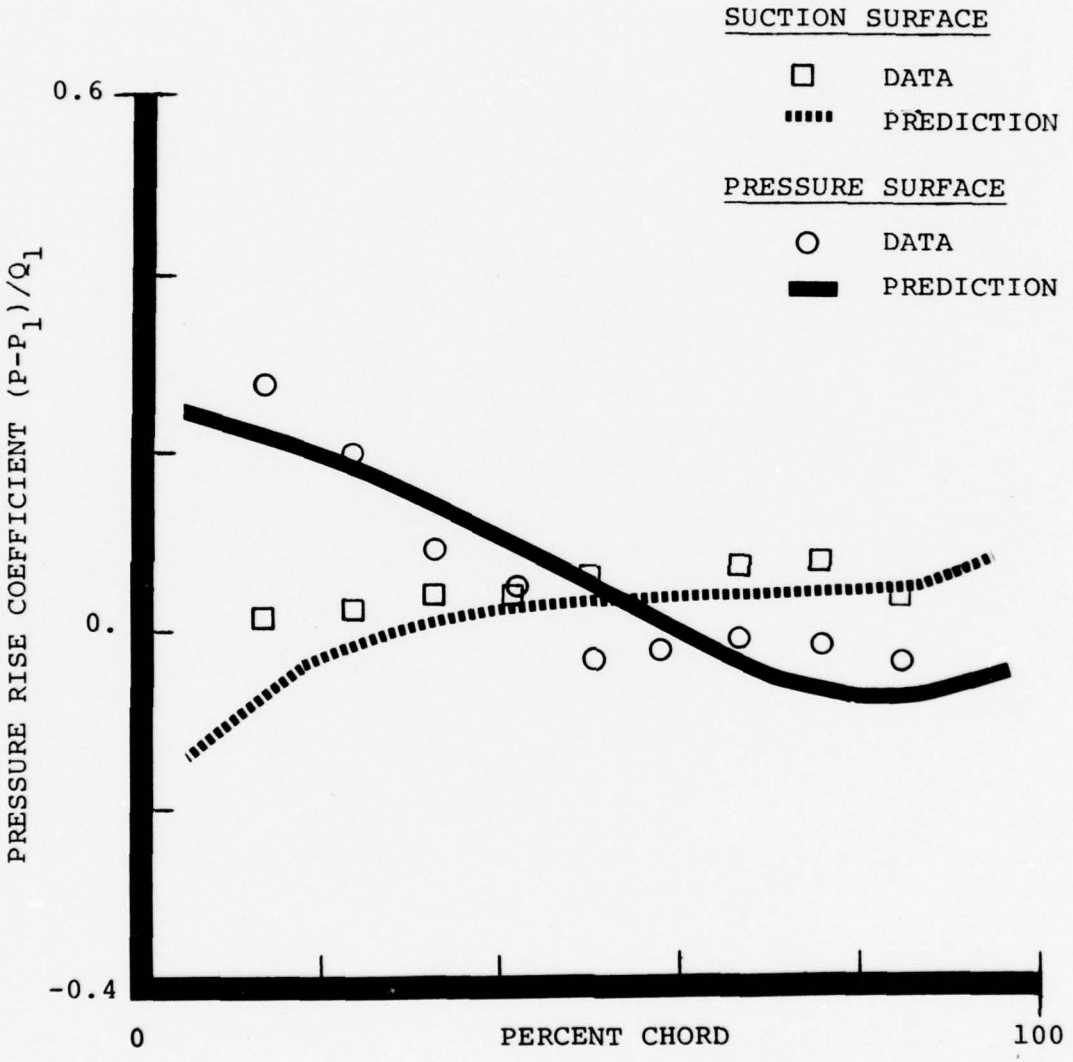

FIGURE 16. MCA AIRFOIL SURFACE STEADY-STATE AERODYNAMIC PERFORMANCE AND CORRELATION WITH THEORY

good near to the leading and trailing edges, regions where the analysis does not accurately model the profile of the airfoil. Also, as previously noted, the current flutter aerodynamic model assumes a uniform steady flow field with small perturbations generated by the harmonic oscillations of zero thickness flat plate cascaded airfoils. Thus Figure 16 demonstrates clearly the differences between this uniform steady flow of the model and the actual steady flow field.

The effect of aerodynamic loading on the time-variant aerodynamics on the suction surface of this MCA airfoil cascade is demonstrated in Figure 17. As seen, increased cascade static pressure ratio generally results in an increased phase lag over the cambered portion of the suction surface. The chordwise trend of the suction surface unsteady pressure coefficient data is to decrease in the direction of the trailing edge. The data is increased significantly in value over the prediction for the front of the surface, decreasing in value and generally approaching the flat plate prediction near the trailing edge. This is an interesting contrast to the phase lag data in that they correlated well with the flat plate prediction over the front portion of this surface.

Figure 18 presents the analogous data-theory correlation on the pressure surface. The time-variant phenomena on this

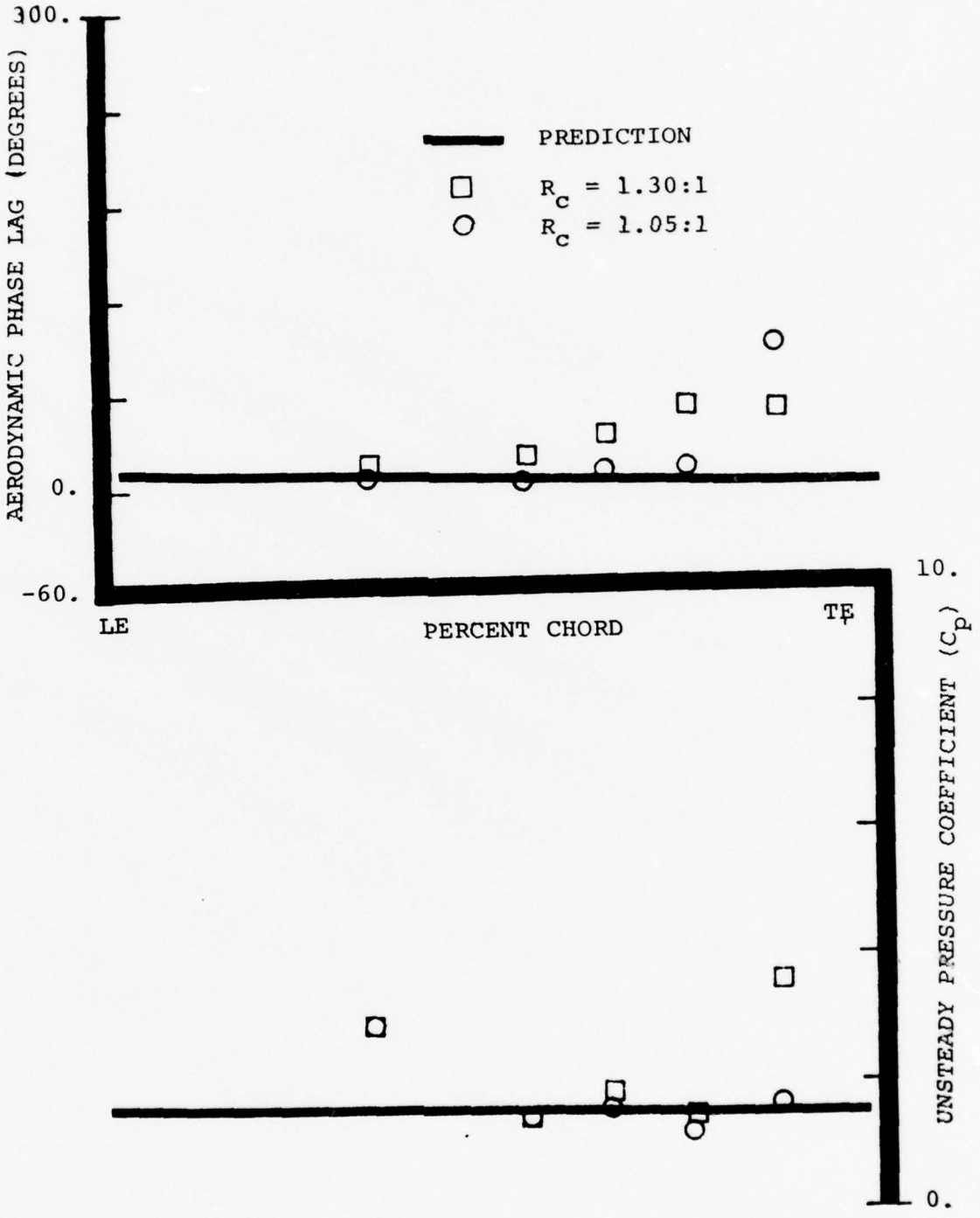

FIGURE 17. MCA AIRFOIL CASCADE TORSION MODE SUCTION SURFACE UNSTEADY CASCADE DATA AND CORRELATION WITH THEORY

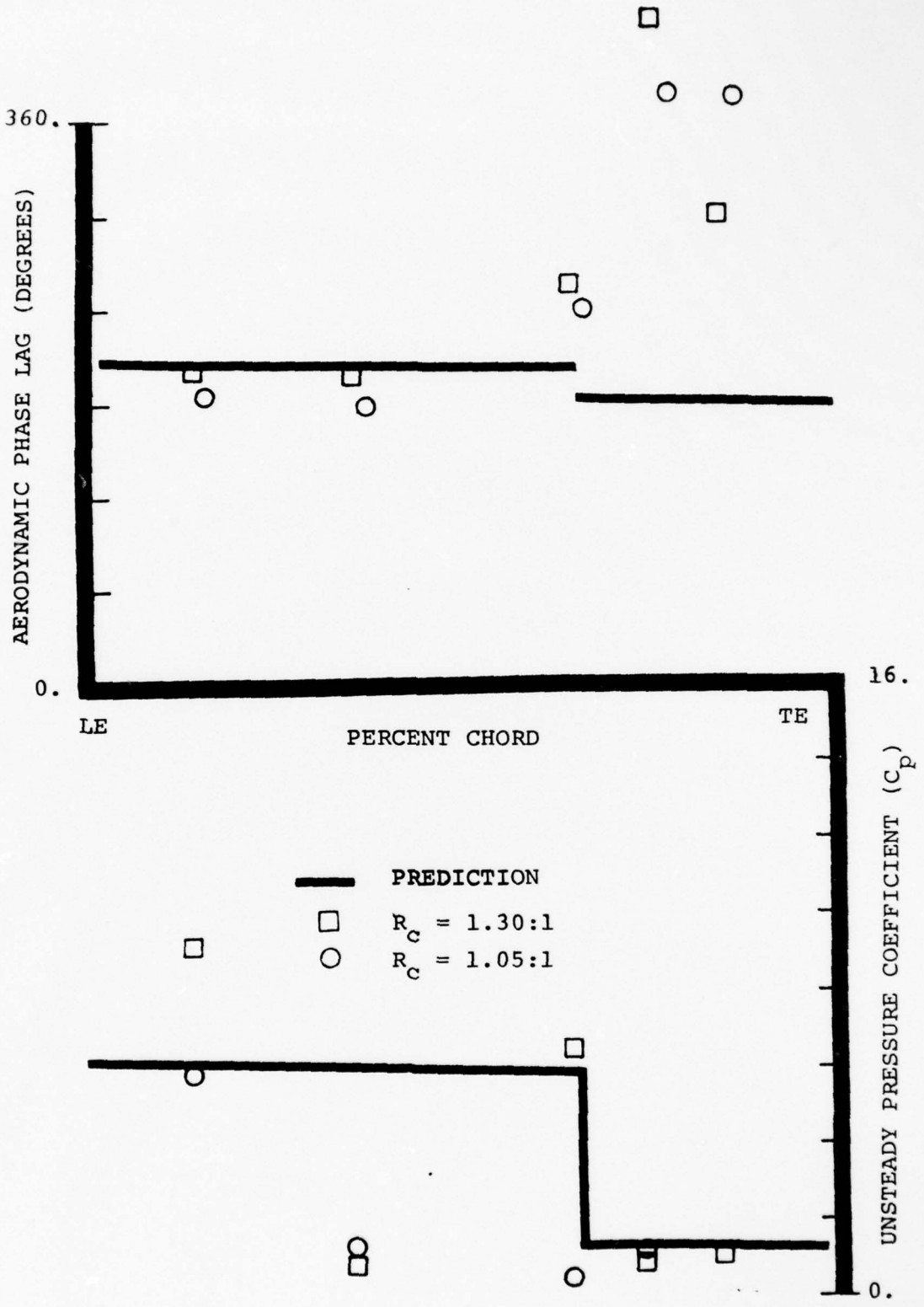

FIGURE 18. MCA AIRFOIL CASCADE TORSION MODE PRESSURE SURFACE UNSTEADY CASCADE DATA AND CORRELATION WITH THEORY

surface are extremely complex as a cambered airfoil surface with two impinging shock waves are involved. Generally the aerodynamic phase lag data exhibits some correlation with the flat plate cascade prediction over the front portion of the pressure surface. For the example shown, the value of the aerodynamic phase lag approaches 360^{o} in the trailing edge region. This may be attributable to the physical phenomena not modeled in the state-of-the-art flat plate cascade analysis. For example, the analysis does not predict the pressure surface impingement of the shock wave originating at the trailing edge of the adjacent airfoil. Also, the steady flow field is modeled as a uniform flow with small unsteady perturbations superimposed, as previously discussed.

Overall, the unsteady pressure coefficient data on the pressure surface shows a relatively large decrease in value between the leading edge and the second chordwise data points, 14.0 percent and 34.5 percent chord, with this second data point demonstrating reasonable agreement with the flat plate prediction. The 65 percent chord data point is located in the immediate vicinity of the impinging trailing edge shock wave, hence the scatter exhibited by the data at this chordwise location between the various interblade phase angle cases.

Over the approximate aft 40 percent of the pressure surface, behind the trailing edge shock intersection, the unsteady pressure coefficient data is in reasonable agreement with the flat plate cascade prediction. Also, as indicated, increased cascade static pressure ratio generally results in an increased aerodynamic phase lag on the pressure surface, analogous to the suction surface results previously discussed.

CASCADE 4

This investigation was directed at extending the range of unsteady supersonic cascade data by developing the necessary new experimental techniques and then obtaining relevant translation mode cascade data. In particular, the fundamental time-variant translation mode aerodynamics are determined for the first time for a classical airfoil cascade in a supersonic inlet flow field.

To achieve realistic reduced frequency values, maintain a two-dimensional airfoil mode shape, and also maximize the imparted airfoil oscillatory amplitude for a given input driving power, unique airfoils fabricated from graphite/epoxy composite material were necessary. The airfoils were fabricated from a combination of pre-impregnated Kevler cloth and graphite mat injected with epoxy resin under pressure into a booking mold.

Cloth fiber orientation was controlled to meet prescribed torsional and bending stress requirements while maintaining a low density and a high modulus of elasticity.

To maintain the desired overall composite material properties with no degradation of the airfoil surface contours, provisions for dynamic instrumentation were embedded in one airfoil during fabrication. This involved molding the dynamic pressure transducer lead wires into the airfoil as part of the lay-up and molding process. The ends of the lead wires were then exposed and the transducers attached. Flush-mounted Kulite dynamic pressure transducers were staggered across the span of the airfoil on both the pressure and suction surfaces. Figure 19 presents a view of this unique dynamically instrumented airfoil.

With the steady-stage periodicity established and the cascade performance determined, the airfoil cascade was harmonically oscillated in a translation mode at a reduced frequency value equal to 0.20. Specified interblade phase angles were investigated and at selected points, the cascade static pressure ratio was increased from the nominal 1.00:1 to 1.30:1.

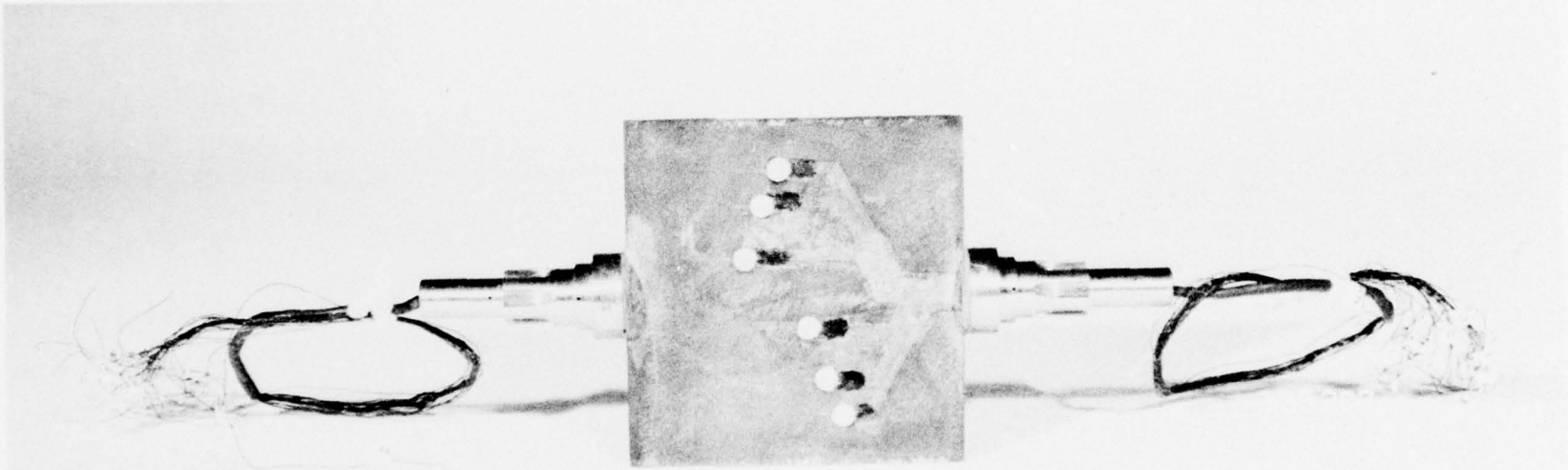

FIGURE 19. DYNAMICALLY INSTRUMENTED GRAPHITE/EPOXY COMPOSITE CLASSICAL AIRFOIL

An example of these unique chordwise pressure and suction surface translation mode data together with the corresponding predictions are presented in Figure 20. As seen, the time-variant suction surface data are seen to generally exhibit very good correlation with the predictions. The aerodynamic phase lag and unsteady pressure coefficient data are both nearly constant in the chordwise direction, with the theory predicting an approximate 60^{o} greater lag than characteristic of the data.

The time-variant pressure surface data also generally exhibit very good correlation with the theory. Both the aerodynamic phase lag and dynamic pressure coefficient data and prediction remain nearly constant in the chordwise direction between the leading edge and the mid-chord region shock wave intersection location on this surface. The theory predicts this intersection location to be at approximately 70% of the chord, with the data indicating a shock in the region between the 60% and 75% chord transducer locations.

An interesting trend was also noted in the aerodynamic phase lag data-theory correlation on the pressure surface in the region between the leading edge and the shock intersection for both values of the pressure ratio which were investigated. In particular, in this region, as the interblade phase angle

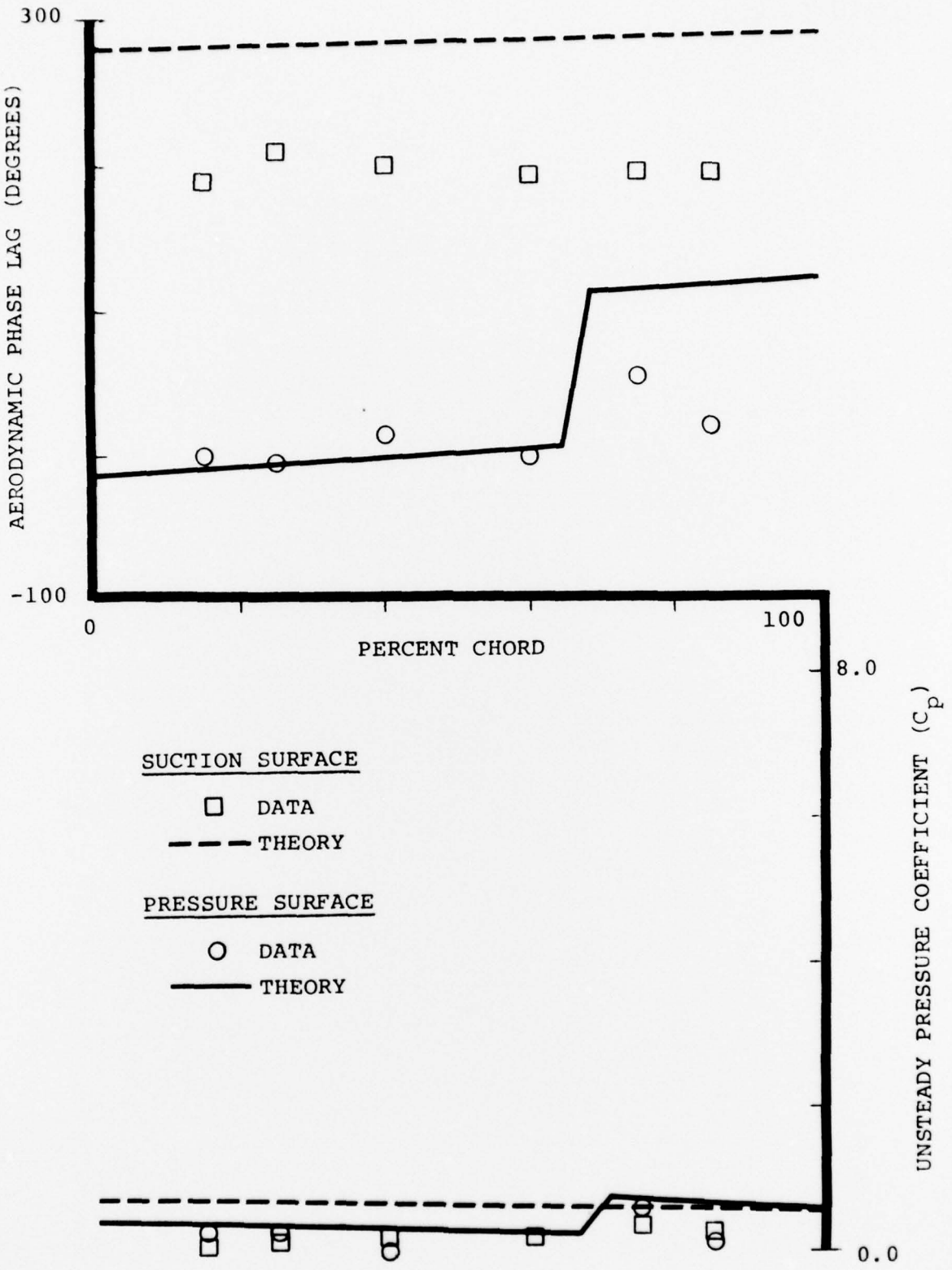

FIGURE 20. TRANSLATION MODE CLASSICAL AIRFOIL CASCADE DATA-THEORY CORRELATION

is decreased and attains larger negative values, the phase lag data decreases as compared to the prediction, with the best data-theory correlation obtained at a 0° interblade phase angle value.

PUBLICATIONS RESULTING FROM ONR SPONSORED RESEARCH

1. Fleeter, S., McClure, R. B., Sinnet, G. T., and Holtman, R. L., "Unsteady Supersonic Inlet Cascade Aerodynamics — A Schlieren Study", 87th Meeting of the Acoustical Society of America, April 1974.

2. Fleeter, S., McClure, R. B., Sinnet, G. T., and Holtman, R. L., "The Torsional Flutter Characteristics of a Cantilevered Airfoil Cascade in a Supersonic Inlet Flow Field with a Subsonic Axial Component", AIAA Paper No. 74-530. June 1974.

3. Fleeter, S., McClure, R. B., Holtman, R. L. and Sinnet, G. T., "A Unique Supersonic Inlet Unsteady Aerodynamic Cascade Experiment", AIAA Paper No. 74-622, July 1975.

4. Fleeter, S., McClure, R. B., Sinnet, G. T. and Holtman, R. L., "Research on Aeroelastic Phenomena in Airfoil Cascades — Supersonic Inlet Torsional Flutter", Office of Naval Research Technical Report, DDA EDR 8297, September 1974.

5. Fleeter, S., McClure, R. B., Sinnet, G. T., and Holtman, R. L., "Supersonic Inlet Torsional Cascade Flutter", AIAA Journal of Aircraft, Vol. 12, No. 8, August 1975.

6. Fleeter, S., Novick, A. S., and Riffel, R. E., "Supersonic Unsteady Aerodynamic Phenomena in a Controlled Oscillating Cascade", Office of Naval Research Technical Report, DDA EDR 8617, October 1975.

7. Fleeter, S., and Riffel, R. E., "An Experimental Investigation of the Unsteady Aerodynamics of a Controlled Oscillating MCA Airfoil Cascade", Office of Naval Research Technical Report, DDA EDR 9028, December 1976.

8. Fleeter, S., Novick, A. S., Riffel, R. E. and Caruthers, J. E., "An Experimental Investigation of the Unsteady Aerodynamics in a Controlled Oscillating Cascade", ASME Journal of Engineering for Power, Vol. 99, No. 1, January 1977.

9. Fleeter, S. and Riffel, R. E., "Aerodynamic Phenomena in an Oscillating Transonic MCA Airfoil Cascade Including Loading Effects", AGARD Symposium on Unsteady Aerodynamics, AGARD-CPP-227, September 1977.

10. Fleeter, S., Riffel, R. E., Lindsey, T. H., and Rothrock, M. D., "An Experimental Investigation of the Unsteady Aerodynamics of a Classical Airfoil Cascade in Translation", Office of Naval Research Technical Report, DDA EDR 9477, April 1978.

11. Fleeter, S., Riffel, R. E., Lindsey, T. H., and Rothrock, M. D., "Time-Variant Translation Mode Aerodynamics of a Classical Transonic Airfoil Cascade", AGARD Propulsion and Energetics Panel Symposium on Stresses, Vibrations, Structural Integration and Engine Integrity, October, 1978.

Recipient	No. of Copies
Director Power Program Material Sciences Division Office of Naval Research Department of the Navy 800 North Quincy Street Arlington, Virginia 22217	(1)
Chief of Naval Research Department of the Navy Washington, D.C. 20360 Attn: Mr. J. R. Patton, Jr., Code 473	(1)
Director U.S. Naval Research Laboratory Washington, D.C. 20390 Attn: Library, Code 2029 (ONRL)	(6)
Director U.S. Naval Research Laboratory Washington, D.C. 20390 Attn: Technical Information Division	(6)
Defense Documentation Center Building 5 Cameron Station Alexandria, Virginia 22314	(12)
Commander Naval Air Systems Command Department of the Navy Washington, D.C. 20360	
Attn: Mr. R. R. Brown, Code 53673	(1)
Mr. I. Silver, Code 330	(1)
Dr. H. Rosenwasser, Code 310C	(1)
Technical Library Division, Code 604	(1)

Recipient	No. of Copies
Commander Naval Ship Systems Command Department of the Navy Washington, D.C. 20360 Attn: Mr. R. R. Peterson, Code 03413 Mr. C. Miller, Code 6146 Technical Library	 (1) (1) (1)
Commanding Officer U.S. Army Research Office Box CM, Duke Station Durham, North Carolina 27706 Attn: ORDOR-PC	 (1)
Director National Aeronautics and Space Administration Headquarters Washington, D.C. 20546 Attn: Division Research Information	 (1)
Office of the Assistant Secretary of Defense (R & D) Room 3E1065 - The Pentagon Washington, D.C. 20301 Attn: Technical Library	 (1)
General Motors Corporation Allison Division Indianapolis, Indiana 46206 Attn: Director of Engineering	 (1)
National Aeronautics and Space Administration Lewis Research Center 21000 Brookpark Road Cleveland, Ohio 44135	 (2)
Commander U.S. Naval Ordnance Laboratory White Oak Silver Spring, Maryland 20910 Attn: Library	 (1)

Recipient	No. of Copies
Commander Naval Weapons Center China Lake, California 93555 Attn: Technical Library	(1)
Commander Wright Air Development Center Wright-Patterson Air Force Base, Ohio 45433 Attn: WCLPN-1, WCACD, WCLPS-1	(3)
Officer in Charge Naval Ship Engineering Center Philadelphia Division Philadelphia, Pennsylvania 19112 Attn: Code 6700 Technical Library	(1) (1)
Superintendent U.S. Naval Postgraduate School Monterey, California 93940 Attn: Professor Vavra Library, Code 0212	(1) (1)
Commander Naval Ordnance Systems Command Department of the Navy Washington, D.C. 20360 Attn: Mr. B. Drimmer, Code 033	(1)
Naval Ship Research and Development Center Annapolis, Maryland 21402 Attn: Library, Code A214	(1)
Naval Undersea Warfare Center 3202 East Foothill Boulevard Pasadena, California 91107 Attn: Technical Library	(1)
Naval Applied Science Laboratory Flushing and Washington Avenues Brooklyn, New York 11251 Attn: Technical Library, Code 222	(1)

Recipient	No. of Copies
Bureau of Naval Personnel Department of the Navy Washington, D.C. 20370 Attn: Technical Library	(1)
U.S. Naval Weapons Laboratory Dahlgren, Virginia 22448 Attn: Technical Library	(1)
Director, Project SQUID Jet Propulsion Center School of Mechanical Engineering Purdue University Lafayette, Indiana 47907	(1)
Army Missile Command Research and Development Directorate Redstone Arsenal, Alabama 35809 Attn: Propulsion Laboratory	(1)
Commander U.S. Air Force Systems Command Andrews Air Force Base Silver Hill, Maryland 20331	(1)
Commander Air Force Aero Propulsion Laboratory Wright-Patterson Air Force Base Dayton, Ohio 45433	(1)
Commander Air Force Rocket Propulsion Laboratory Edwards Air Force Base, California 93523	(1)
Naval Missile Center Point Mugu, California 93041 Attn: Technical Library Code 5632.2	(1)

Recipient	No. of Copies
Headquarters Naval Material Command Special Projects Office Washington, D.C. 20360 Attn: Technical Library	(2)
Commander Air Force Office of Scientific Research 1400 Wilson Boulevard Arlington, Virginia 22209 Attn: J. F. Masi M. Rogers	(1)
Director of Defense Research and Engineering Technical Library Room 3C128 - The Pentagon Washington, D.C. 20301 Attn: Propulsion Technology	(1)
Chief of Research and Development Headquarters, Department of the Army Washington, D.C. 20310 Attn: Dr. S. J. Magram Physical and Engineering Division	(1)
Dr. Sanford Fleeter Chaffee Hall Purdue University West Lafayette, Indiana 47907	(1)

UNCLASSIFIED

SECURITY CLASSIFICATION OF THIS PAGE (When Data Entered)

REPORT DOCUMENTATION PAGE		READ INSTRUCTIONS BEFORE COMPLETING FORM
1. REPORT NUMBER EDR 9575	2. GOVT ACCESSION NO.	3. RECIPIENT'S CATALOG NUMBER
4. TITLE (and Subtitle) Research on Aeroelastic Phenomena in Airfoil Cascades – Final Summary Report		5. TYPE OF REPORT & PERIOD COVERED Final Report 6. PERFORMING ORG. REPORT NUMBER
7. AUTHOR(s) Sanford Fleeter		8. CONTRACT OR GRANT NUMBER(s) N00014-72-C-0351
9. PERFORMING ORGANIZATION NAME AND ADDRESS Detroit Diesel Allison Division General Motors Corporation Indianapolis, Indiana 46206		10. PROGRAM ELEMENT, PROJECT, TASK AREA & WORK UNIT NUMBERS N094-369
11. CONTROLLING OFFICE NAME AND ADDRESS Power Branch Office of Naval Research - Code 473 Arlington, Virginia 22217		12. REPORT DATE August 1978 13. NUMBER OF PAGES 52
14. MONITORING AGENCY NAME & ADDRESS(if different from Controlling Office)		15. SECURITY CLASS. (of this report) Unclassified 15a. DECLASSIFICATION/DOWNGRADING SCHEDULE

16. DISTRIBUTION STATEMENT (of this Report)

This document has been approved for public release and sale; its distribution is unlimited.

17. DISTRIBUTION STATEMENT (of the abstract entered in Block 20, if different from Report)

18. SUPPLEMENTARY NOTES

19. KEY WORDS (Continue on reverse side if necessary and identify by block number)

Flutter, Aeroelasticity, Turbomachinery, Aerodynamics, Experimental Techniques, Cascades, Dynamic Measurements

20. ABSTRACT (Continue on reverse side if necessary and identify by block number)

The advent of high tip, high [illegible], blading in the fan stages of advanced gas turbine engines has led to the recognition of a new type of blading instability – unstalled supersonic flutter. As a result, a concerted effort to develop an appropriate predictive mathematical model has taken place. To determine the range of validity and to direct refinements to the basic flow model, fundamental supersonic oscillating cascade data are required.

DD FORM 1 JAN 73 1473 EDITION OF 1 NOV 65 IS OBSOLETE

UNCLASSIFIED

SECURITY CLASSIFICATION OF THIS PAGE (When Data Entered)

This is the final summary report for an experimental research program directed at obtaining these unique time-variant aerodynamic data. The approach involved harmonically oscillating dynamically instrumented 2-D rectilinear cascades of airfoils in a supersonic inlet flow field, with the unsteady operation of the cascade computer controlled. Data were obtained in both torsion and translation over a range of steady and time-variant aerodynamic conditions. All of these data were then correlated with predictions obtained from a current state-of-the-art model.